

## REVIEW

View Article Online

View Journal | View Issue

Cite this: *Inorg. Chem. Front.*, 2024, **11**, 1339

# Advancing biomedical applications of polyoxometalate-based metal–organic frameworks: from design to therapeutic potential

Lijin Wang, †<sup>a</sup> Pengyu Dai, †<sup>a</sup> Hongli Ma, \*<sup>b</sup> Tiedong Sun \*<sup>a</sup> and Jinsong Peng \*<sup>a</sup>

Polyoxometalate-based metal–organic frameworks (POMOFs) are novel materials composed of polyoxometalates (POMs) and metal–organic frameworks (MOFs), which are widely used in biomedical research. Synthesis strategies for POMOF materials predominantly utilise liquid-phase self-assembly *via* diverse methodologies and solid-phase self-assembly facilitated by mechanical grinding. Additionally, POMOF materials can be modified to enhance their efficacy through enhancements in catalytic activity and structural refinement. This review article summarises the common design, synthesis, and modification strategies of POMOF materials suitable for biomedical applications. The review further elucidates the unique properties of POMOF materials, regulatability, stability, and multifunctionality, which distinctly exceed those of other biomedical materials. Subsequently, the review is centred on applying POMOF biosensors classified by colourimetric and electrochemical methods and their multiple roles in biomedical therapy fields. Finally, we introduce the challenges faced by POMOFs in terms of synthesis methods and, using conditions, propose potential solutions and summarise the future development potential of POMOFs in the field of biomedical detection and therapy.

Received 22nd November 2023,

Accepted 16th January 2024

DOI: 10.1039/d3qi02414h

rsc.li/frontiers-inorganic

## 1 Introduction

MOFs represent a burgeoning class of porous functional materials wherein metal ions (predominantly transition metal ions) intricately coordinate with organic ligands to form a robust framework.<sup>1</sup> The establishment of these coordination bonds results in a highly versatile and regulatable structure,

<sup>a</sup>College of Chemistry, Chemical Engineering and Resource Utilization, Northeast Forestry University, Harbin, 150040, China. E-mail: tiedongsun@nefu.edu.cn, jspeng1998@nefu.edu.cn

<sup>b</sup>The First Hospital of Suihua, Suihua, 152000, China.

E-mail: mahongli2010ok@163.com

†These authors contributed equally to this work and should be considered co-first authors.



Lijin Wang

Lijin Wang received her B.S. degree in Chemistry from the Northeast Forestry University in 2023 under the guidance of Prof. Jinsong Peng. Her research focuses on the biomedical application of POMOF nanomaterials based on probe and catalysis, and photothermal therapy (PTT) combined with starvation therapy in collaborative diagnosis and treatment and prescription of multiple tumours, as well as the structure–activity relationship of camptothecin and its derivatives in tumour therapy.



Pengyu Dai

Pengyu Dai received his B.S. and B.Eng. degrees in Chemistry and Computer Science from the Northeast Forestry University in 2023. His research work mainly involves improving the catalytic activity of nanozymes and enhancing the targeting of nanozymes for the diagnosis and therapy of diseases. His most recent research project is materials research on black phosphorus nanoribbons.

rendering MOFs promising candidates for diverse applications in advanced materials.<sup>2</sup> MOFs exhibit precise regulation of pore sizes within the micron to nanometer scale range.<sup>3</sup> The remarkable attributes of MOFs include an exceedingly high specific surface area, customisable pore volume, regulatable pore sizes, and adjustable surface properties, imparting great promise for multifaceted applications in adsorption, separation, and catalysis.<sup>4</sup> The extraordinary array of properties exhibited by MOFs has led to their burgeoning applications in the field of biomedicine.<sup>5</sup> To propel the advancement of MOFs in biomedicine, several challenges and complexities persist in MOF materials research.<sup>6</sup> Notably, enhancing the stability of MOFs remains imperative to meet application demands across diverse conditions. At the same time, achieving successful integration and synergy with computational and other disciplines will enable MOFs for practical applications.<sup>7</sup> Furthermore, the ongoing development and refinement of synthesis and modification methodologies are essential to expand the prospects of MOFs in biomedicine further.<sup>8</sup>

POMs are a subclass of metal oxides consisting of multiple metal oxide clusters with unique physical and chemical properties that generate dynamic micron to nanometer-scale structures.<sup>9</sup> According to the structure of POMs, POMs can be divided into six main types: Keggin, Wells–Dawson, Silverton, Waugh, Lindqvist, and Anderson. Various methods can tune the structure and properties of POMs.<sup>10</sup> The regulatable acidity and solubility of POMs make them an important catalyst for a wide range of organic reactions.<sup>11</sup> The acidic and redox properties of POMs can be fine-tuned by changing their constituent elements, thereby tuning their catalytic activity according to different scenarios.<sup>12</sup> POMs can also be combined with organic molecules to form organic–inorganic hybrid materials, which can achieve the modulation of their optical, electrical, and magnetic properties, thus expanding their applications in materials science and nanotechnology.<sup>13</sup> POMs also have good multi-electron redox properties and can undergo redox transformations under mild conditions, making them adaptable to

various applications. POM anions are a group of inorganic building blocks with Lewis and Brønsted acidity that can be used as efficient solid acid catalysts for various organic reactions.<sup>14</sup> The multi-electron redox properties of POMs also make them an ideal electrocatalyst for photoelectrochemistry, capacitors, and other applications.<sup>15</sup> The regulatability and multi-electron redox attributes of POMs are now making notable strides in the realm of antibacterial and antitumour biomedical treatments, exemplifying their burgeoning applications in this field.<sup>16</sup>

The convergence of POM and MOF materials has emerged as a prominent and compelling research frontier, driven by their individual outstanding properties.<sup>17</sup> MOFs with high porosity provide a platform for good dispersion of POMs and improve the exposure of active sites. Various organic ligands can be selected to design MOFs with the desired structure and fixed pore size to meet their requirements for encapsulating POMs.<sup>18</sup> The multicomponent synergistic effect between the two components can produce excellent composite properties. Currently, POMOF materials exhibit exceptional adsorption properties, rendering them ideal loading materials for sensor applications. Primarily, they facilitate the selective loading of specific substance components, enabling the sensing of various physical quantities, including pH and temperature. Additionally, POMOF materials exhibit enzyme-like activity for colourimetric detection and manifest electrochemical catalytic activity for electrochemical sensing purposes. This multifaceted functionality positions POMOF materials as a promising candidate for advancing sensor technologies.<sup>19</sup> POMOF materials are also used in biomedical therapy because the vigorous enzyme-like activity can control the balance of reactive oxygen species (ROS) in the body, thus treating tumours and inflammation. Moreover, the POMOFs platform presents commendable mechanical properties, making it an appealing medium for drug encapsulation and delivery while also serving as an effective enzyme carrier to augment therapeutic interventions. In summary, the unique properties (regulabil-



**Hongli Ma**

*Hongli Ma received her master's degree in the Clinical Major at Jilin University in 2013. Following her academic achievement, she undertook her professional engagement at the Obstetrics and Gynecology Department of the First Hospital of Suihua. In October 2021, she began her teaching duties, and in February 2022, she became the deputy director of the Second Gynecology Department. She primarily engages in the research of anti-tumour drugs and is skilled in diagnosing and treating common gynaecological diseases.*



**Tiedong Sun**

*Tiedong Sun received his Ph.D. degree from the Harbin Institute of Technology in 2016. He studied at Yale University as an international exchange student and then joined Northeast Forestry University as a faculty member. He was promoted to associate professor in 2017 and then promoted to professor in 2023, now at the College of Chemistry, Chemical Engineering and Resource Utilization, Northeast Forestry University. His research work focuses on the biomimetic synthesis of nanozymes and their biomedical applications.*

ity, stability, and multifunctionality) of POMOF materials warrant continued scrutiny and exploration within the realm of biomedical research, accentuating their potential for transformative advancements in drug delivery and medical therapies.<sup>20</sup> Table 1 demonstrates the biomedical applications of POMOF materials. Fig. 1 encapsulates a visual overview of POMOF materials deployed in the biomedical therapy field.

This review presents a comprehensive review of the burgeoning applications of POMOF materials in biomedicine. Firstly, the synthesis strategies, encompassing liquid-phase self-assembly and solid-phase self-assembly methods, are thoroughly elucidated. Subsequently, the modification strategies applied to POMOFs, involving catalytic activity and structural refinement, are detailed. This review also introduces the unique properties of POMOFs based on regulatability, stability, and multifunctionality. POMOFs in biosensing are classified according to their colourimetric and electrochemical detection capabilities, which are rooted in their electrocatalytic activity (EA). Moreover, the potential of POMOFs in biomedical treatment is explored, encompassing their applications in antibacterial and antitumour aspects. Lastly, the therapeutic prospects of POMOFs in biomedical applications are astutely anticipated, highlighting promising avenues for future research and development.

## 2 Synthesis strategies

As innovative synthesis technologies rapidly advance, POMOF preparation methodologies have diversified significantly.<sup>56</sup> This review focuses on the strategic synthesis of POMOFs, delivering a systematic elucidation of their developmental trajectory. For POMOF materials with biomedical applications, two main types can be distinguished, the first with POMs as part of a framework and the second with POMs encapsulated within the cavities of MOFs. This objective is realised by employing a self-assembly strategy.<sup>57</sup> The self-assembly strategy is pivotal in POMOF synthesis, grounded on the principle of molecules or atoms autonomously organising into ordered structures *via* local interactions.<sup>58</sup> This approach is advan-

tageous due to its operational simplicity, yet it exhibits considerable dependence on reaction conditions, including the concentration and type of metal oxide anions, heteroatoms, pH, ionic strength, reducing agents, ligands, and temperature.<sup>59</sup> Achieving full control of the synthesis of POMOF structures continues to be a formidable challenge within POMOF applications. In POMOF synthesis, self-assembly is primarily categorised into two types: solid-phase self-assembly and liquid-phase self-assembly, both of which are delineated subsequently.<sup>60</sup>

### 2.1 Liquid-phase self-assembly strategy

Within the liquid-phase self-assembly process for POMOFs, metal precursors and organic ligands coalesce in solution, utilising intermolecular interactions present in the solvent like “hydrogen bonding, coordination bonds, and van der Waals forces” to facilitate self-assembly.<sup>61</sup> This method’s merit lies in the precise controllability of POMOF’s structure and properties by altering the solvent, temperature, pH, and other reaction conditions.<sup>62</sup> Conversely, the drawback is that the reaction kinetics of POMOF liquid-phase self-assembly can be intricate, necessitating extensive experimentation and theoretical calculations to preclude side reactions. Liquid-phase self-assembly is crucial for synthesising POMOFs with tailored pore structures and functionalities, finding extensive applications in catalysis, targeted transport, drug release, and various other domains.<sup>63</sup> For biomedical applications of POMOFs, liquid-phase self-assembly predominantly occurs *via* hydrothermal or solvothermal synthesis methods.<sup>64</sup> The production of specially functionalised POMOF materials necessitates hydrothermal or solvothermal synthesis under high-pressure conditions as a component of the one-pot process.<sup>65</sup>

**2.1.1 Hydrothermal or solvothermal method.** The primary approaches are the conventional hydrothermal and solvothermal synthesis methods, frequently employed in laboratory syntheses.<sup>66</sup> Xu *et al.* prepared NiMo<sub>6</sub>@ZIF-67 materials for the detection of L-cysteine, introducing pre-existing ZIF-67 into a methanol solution containing Co(NO<sub>3</sub>)<sub>2</sub>·6H<sub>2</sub>O and NiMo<sub>6</sub>, and stirred it gently with heat until NiMo<sub>6</sub> was undetectable by UV-Vis in the solution, indicating completion of self-assembly.<sup>30</sup> While these hydrothermal and solvothermal techniques facilitate rapid crystal growth, they necessitate subsequent modifications before application.

**2.1.2 Ultrasonic drive method.** In the synthesis of Cu<sub>18</sub>PW<sub>12</sub>/SWNTs materials applied to L-cysteine, Li *et al.* employed an ultrasonically driven functionalisation approach to enhance liquid-phase self-assembly.<sup>25</sup> Initially, two novel [PW<sub>12</sub>O<sub>40</sub>]<sup>3-</sup> based Cu-triazole (trz) MOFs were synthesised successfully. Subsequently, POMs, MOFs, and SWNTs (single-walled carbon nanotubes) were amalgamated in methanol utilising a straightforward ultrasonic-driven periodic functionalisation strategy, followed by drying to procure the final product. This strategy was also adopted by Zhou *et al.* in the creation of PAZ@SWCNTs-COOH materials aimed at dopamine detection.<sup>33</sup> The utilisation of ultrasonic-driven techniques facili-



Jinsong Peng

*Jinsong Peng graduated from Southwest University for Nationalities in 2002 and received his Ph.D. in 2007 from the Chengdu Institute of Organic Chemistry, Chinese Academy of Sciences. He became an associate professor at Northeast Forestry University in 2007 and was promoted to full professor in 2018. His current research interest is focused on the design, synthesis and discovery of novel anti-tumor drugs.*

Table 1 Representative biomedical applications for POMOF materials

Applications	POMOFs	Abbreviations	Types (POMs)	Activities	Synthesis	Ref.
pH	{Mn(3-dpye) <sub>0.5</sub> [CrMo <sub>6</sub> (OH) <sub>6</sub> O <sub>18</sub> ](H <sub>2</sub> O)}·(3-H <sub>2</sub> dpye) <sub>0.5</sub>	C <sub>14</sub> H <sub>23</sub> CrMnMo <sub>6</sub> N <sub>4</sub> O <sub>27</sub>	Anderson	Carrier	One-pot	21
Temperature	Eu, TbPOM@MOF	Eu, TbPOM@MOF	Keggin	Carrier	Hydrothermal	22
Temperature	EuW <sub>10</sub> @ [Tb <sub>16</sub> (TATB) <sub>16</sub> (DMA) <sub>24</sub> ]-91DMA·108H <sub>2</sub> O	EuW <sub>10</sub> @Tb-TATB-DMA	Weakley	Carrier	Impregnation	23
H <sub>2</sub> O <sub>2</sub>	[Cu <sub>5</sub> (pz) <sub>6</sub> Cl][SiW <sub>12</sub> O <sub>40</sub> ]	CuSiW <sub>12</sub>	Keggin	POD	One-pot	24
L-Cysteine	[Cu <sub>18</sub> (trz) <sub>12</sub> Cl <sub>3</sub> (H <sub>2</sub> O) <sub>2</sub> ][PW <sub>12</sub> O <sub>40</sub> ]/SWNTs	Cu <sub>18</sub> PW <sub>12</sub> /SWNTs	Keggin	POD	Ultrasound	25
AA&H <sub>2</sub> O <sub>2</sub>	[Ag <sub>3</sub> (FKZ) <sub>2</sub> (H <sub>2</sub> O) <sub>2</sub> ][H <sub>3</sub> SiW <sub>12</sub> O <sub>40</sub> ]@PPy	AgFKZSiW <sub>12</sub> @PPy	Keggin	POD	One-pot	26
UA	Ag <sub>5</sub> [bimt] <sub>2</sub> [PMo <sub>12</sub> O <sub>40</sub> ]·2H <sub>2</sub> O@PPy	Ag <sub>5</sub> PMo <sub>12</sub> @PPy	Keggin	POD	One-pot	27
AA&H <sub>2</sub> O <sub>2</sub>	[Cu <sub>9</sub> (FKZ) <sub>12</sub> (H <sub>2</sub> O) <sub>8</sub> ][H <sub>3</sub> P <sub>2</sub> W <sub>18</sub> O <sub>62</sub> ] <sub>2</sub> ·4H <sub>2</sub> O/PPy	CuFKZP <sub>2</sub> W <sub>18</sub> /PPy	Wells-Dawson	POD	One-pot	28
CA&H <sub>2</sub> O <sub>2</sub>	[Ni <sub>4</sub> (Trz) <sub>6</sub> (H <sub>2</sub> O) <sub>2</sub> ][SiW <sub>12</sub> O <sub>40</sub> ]·4H <sub>2</sub> O/PDDA-rGO	Ni <sub>4</sub> SiW <sub>12</sub> /PDDA-rGO	Keggin	POD	One-pot	29
L-Cysteine	NiMo <sub>6</sub> @ZIF-67	NiMo <sub>6</sub> @ZIF-67	Anderson	POD	Solvothermal	30
Glc	MIL-100(Fe)@PMo <sub>12</sub> @3DGO	MIL-100@PMo <sub>12</sub>	Keggin	POD	One-pot	31
Glc	MIL-101(Fe)@P <sub>2</sub> W <sub>18</sub> @SWNT	MIL-101@P <sub>2</sub> W <sub>18</sub>	Wells-Dawson	POD	One-pot	32
DA	[Ag <sub>5</sub> (trz) <sub>4</sub> ] <sub>2</sub> [PMo <sub>12</sub> O <sub>40</sub> ]@SWCNTs-COOH	PAZ@SWCNTs-COOH	Keggin	EA	One-pot	33
DA	V <sub>10</sub> O <sub>28</sub> @NU-902	V <sub>10</sub> O <sub>28</sub> @NU-902	Keggin	EA	Impregnation	34
XA	CuMOF <sub>2</sub> W <sub>18</sub>	CuMOF <sub>2</sub> W <sub>18</sub>	Dawson	EA	One-pot	35
L-Cysteine	Mo-POM@HKUST-1	Mo-POM@HKUST-1	Dawson	EA	One-pot	36
H <sub>2</sub> O <sub>2</sub>	[Cu <sub>2</sub> (BTC) <sub>4/3</sub> (H <sub>2</sub> O) <sub>2</sub> ] <sub>6</sub> [H <sub>3</sub> PMo <sub>12</sub> O <sub>40</sub> ]-KB	NENU5-KB	Keggin	EA	One-pot	37
H <sub>2</sub> O <sub>2</sub>	{[Ag <sub>5</sub> bpy <sub>2</sub> Cl <sub>2</sub> ]{As(W <sup>V</sup> ) <sub>2</sub> (W <sup>VI</sup> ) <sub>10</sub> O <sub>40</sub> }}·H <sub>2</sub> O	AsW <sub>12</sub> @MOF	Keggin	EA	Grind	38
H <sub>2</sub> O <sub>2</sub>	[Ag <sub>5</sub> BW <sub>12</sub> O <sub>40</sub> ]@ [Ag <sub>3</sub> (μ-Hbtc)(μ-H <sub>2</sub> btc)] <sub>n</sub>	Ag <sub>5</sub> [BW <sub>12</sub> O <sub>40</sub> ]@Ag-BTC-2	Keggin	EA	Grind	39
H <sub>2</sub> O <sub>2</sub>	{Co <sub>3</sub> Mo <sub>7</sub> O <sub>24</sub> }@ [Ag <sub>4</sub> (μ-Hbtc)(μ-H <sub>2</sub> btc)] <sub>1/2</sub>	Co <sub>3</sub> Mo <sub>7</sub> O <sub>24</sub> @Ag-BTC-2	Keggin	EA	Grind	40
H <sub>2</sub> O <sub>2</sub>	{Ag <sub>4</sub> K <sub>2</sub> P <sub>2</sub> W <sub>18</sub> O <sub>62</sub> }@ [Ag <sub>3</sub> (μ-Hbtc)(μ-H <sub>2</sub> btc)] <sub>n</sub>	Ag <sub>4</sub> K <sub>2</sub> P <sub>2</sub> W <sub>18</sub> O <sub>62</sub> @Ag-BTC- <i>n</i>	Wells-Dawson	EA	Grind	41
H <sub>2</sub> O <sub>2</sub>	CoK <sub>4</sub> [P <sub>2</sub> W <sub>18</sub> O <sub>62</sub> ]@Co <sub>3</sub> (btc) <sub>2</sub>	P <sub>2</sub> W <sub>18</sub> @Co-BTC	Wells-Dawson	EA	Grind	42
H <sub>2</sub> O <sub>2</sub>	[Ag <sub>5</sub> (pz) <sub>6</sub> (H <sub>2</sub> O) <sub>4</sub> ][BW <sub>12</sub> O <sub>40</sub> ]	[Ag <sub>5</sub> (pz) <sub>6</sub> (H <sub>2</sub> O) <sub>4</sub> ][BW <sub>12</sub> O <sub>40</sub> ]	Keggin	EA	One-pot	43
H <sub>2</sub> O <sub>2</sub>	Ni <sub>3</sub> P <sub>2</sub> W <sub>18</sub> O <sub>62</sub> -Ni <sub>3</sub> (BTC) <sub>2</sub>	Ni <sub>3</sub> P <sub>2</sub> W <sub>18</sub> O <sub>62</sub> -Ni <sub>3</sub> (BTC) <sub>2</sub>	Wells-Dawson	EA	Grind	44
H <sub>2</sub> O <sub>2</sub>	Cu <sub>3</sub> [P <sub>2</sub> W <sub>18</sub> O <sub>62</sub> ]@HKUST-1	HRBNU-7	Wells-Dawson	EA	Grind	45
Antitumour	W-POM NCs@HKUST-1	W-POM NCs@HKUST-1	Keggin	POD	Impregnation	46
Antitumour	{ZnW <sub>11</sub> CuO <sub>40</sub> }@ZIF-8 NPs	POM@ZIF-8	Keggin	POD	Hydrothermal	47
Antitumour	POM-CaO <sub>2</sub> @ZIF-8	POM-CaO <sub>2</sub> @ZIF-8	Keggin	POD	One-pot	48
Antitumour	ZIF-8/CQ/POM/HA NPs	ZCPH NPs	Keggin	POD	Solvothermal	49
Antibacterial	[Ag <sub>3</sub> (H <sub>2</sub> O)(L) <sub>2</sub> ](H <sub>2</sub> PMo <sub>12</sub> O <sub>40</sub> )·H <sub>2</sub> O	PMo <sub>12</sub> @MOF	Keggin	POD	One-pot	50
Enzyme therapy	PW <sub>12</sub> @UiO-67	PW <sub>12</sub> @UiO-67	Keggin	Absorbent	One-pot	51
Macrophage	H <sub>2</sub> [β-P(Mo <sup>V</sup> ) <sub>4</sub> (Mo <sup>VI</sup> ) <sub>8</sub> O <sub>40</sub> ]@MIL-101	POM@MIL-101	Keggin	Carrier	One-pot	52
Degradation of antibiotics	H <sub>3</sub> PMo <sub>12</sub> O <sub>40</sub> · <i>n</i> H <sub>2</sub> O@ZIF-67	PMA@ZIF-67	Keggin	Carrier	Impregnation	53
Degradation of antibiotics	PMo <sub>12</sub> O <sub>40</sub> @MIL-101	POM@MIL-101	Keggin	Carrier	Solvothermal	54
Cyt-C	Na <sub>6</sub> [TeW <sub>6</sub> O <sub>24</sub> ]·22H <sub>2</sub> O@ZIF-8	TeW <sub>6</sub> @ZIF-8	Anderson	Carrier	Impregnation	55

tates a more efficacious material integration, thereby augmenting the performance of the resultant POMOF composite.

**2.1.3 One-pot method.** Wang *et al.* also prepared Ag<sub>5</sub>PMo<sub>12</sub>@PPy materials for detecting uric acid through one-pot strategic liquid-phase self-assembly.<sup>27</sup> Dissolve H<sub>3</sub>PMo<sub>12</sub>O<sub>40</sub>, silver nitrate, and NaVO<sub>3</sub> in water and agitate for thirty minutes until homogeneity is achieved. Adjust the pH to roughly 1.75, transfer the blend into a reaction kettle, elevate the temperature to 170 °C, and maintain for four days. Following ancillary post-treatment steps, including filtration, deionised water rinsing, and air-drying, the nascent POMOF product is procured, which, post-enhancement and refinement, is ready for use. Furthermore, numerous POMOF syntheses employ this methodology.

Murinzi *et al.*'s Mo-POM@HKUST-1<sup>36</sup> and Wang *et al.*'s NENU5-KB<sup>37</sup> materials were crafted following a proposed

efficacious pre-synthesis treatment, where the precursors were blended into a gel-like substance before one-pot synthesis. Addressing the three-dimensional network structure engendered by polymerisation or cross-linking in such a manner not only effectually governs the architecture of the synthesised material but also diminishes reliance on organic solvents during the reaction. In the aforementioned synthetic protocol, the system's pH is maintained between 1.75 and 3.4, with the reaction temperature regulated between 120 °C and 180 °C. Although the one-pot approach for liquid-phase self-assembly is straightforward and apt for intricate systems, the matters of raw material utilisation and product purity necessitate additional investigation.<sup>67</sup>

**2.1.4 Impregnation method.** Ho *et al.* employed the dipping technique for liquid-phase self-assembly in fabricating V<sub>10</sub>O<sub>28</sub>@NU-902 materials aimed at dopamine detection,



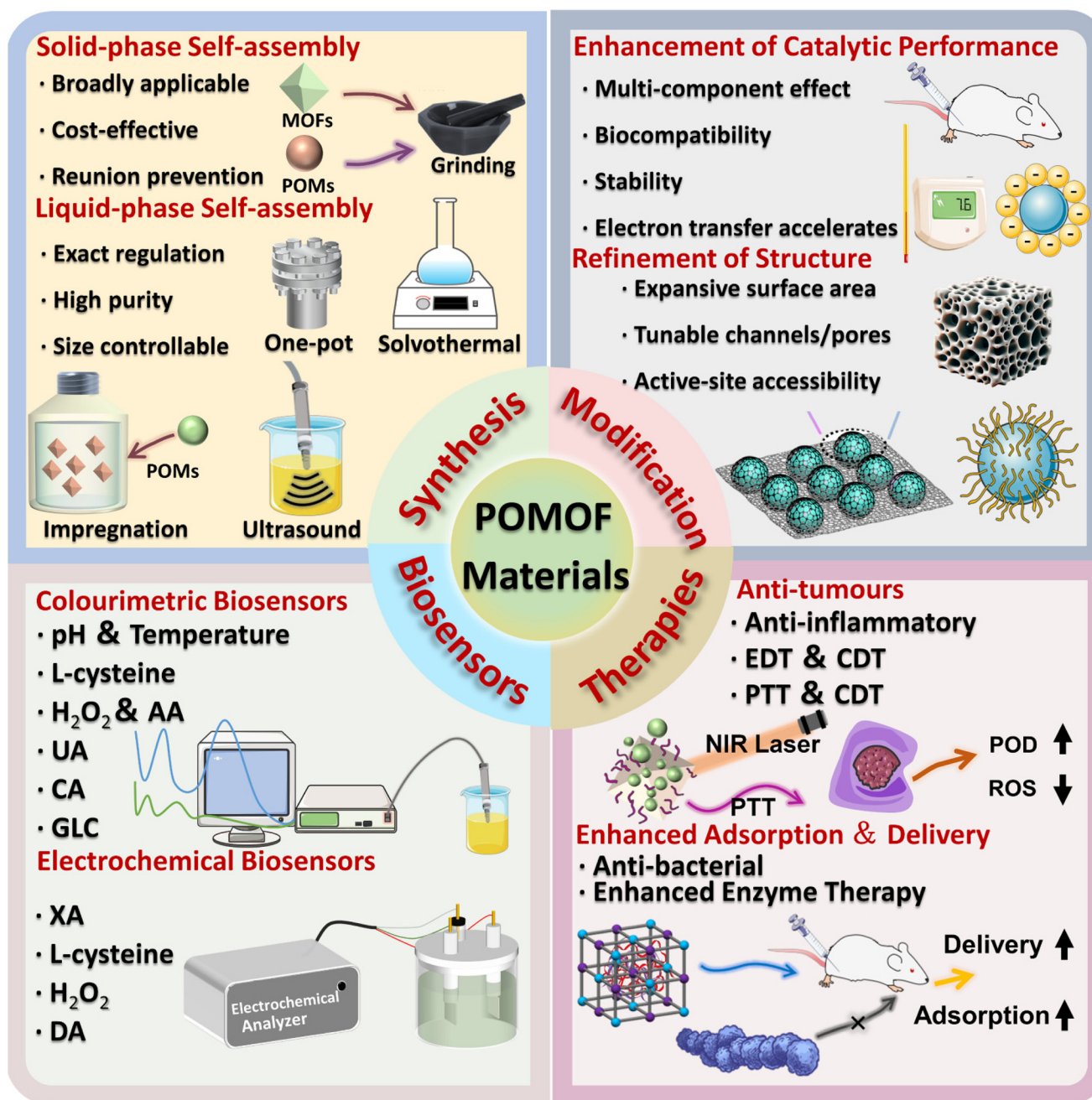


Fig. 1 Summary illustration of POMOF materials used in biomedical fields.

introducing V<sub>10</sub>O<sub>28</sub> into NU-902 within a liquid medium.<sup>34</sup> Specifically, V<sub>10</sub>O<sub>28</sub> has initially dissolved in an acidic aqueous solution at a pH of 4.5, followed by the immersion of pre-existing NU-902 to acquire the POMOFs product, post-impregnation, cleansing, solvent exchange, and drying stages. Impregnation-driven liquid-phase self-assembly facilitates the tailoring of materials to various application demands. However, a drawback is that POMOFs synthesised *via* the impregnation approach exhibit subpar mechanical and chemical stabilities.

Liquid-phase self-assembly is pivotal in the synthesis strategies for POMOF materials, encompassing hydrothermal or

solvothermal techniques, ultrasonic facilitation, impregnation procedures, and one-pot approaches. This strategy permits exact manipulation of POMOF's structure and properties by modulating the solvent, temperature, and pH, among other variables. Nevertheless, the recovery rate of raw materials and the reaction kinetics within this POMOFs synthesis strategy require additional exploration.<sup>68</sup>

## 2.2 Solid-phase self-assembly strategy

Solid-phase self-assembly constitutes a principal synthesis technique for POMOF materials within the biomedical treat-

ment domain. It involves the formation of an ordered structure through interplay among solid substances.<sup>69</sup> This assembly process accentuates physical means, with diverse methods applicable to foster or regulate self-organizational behaviours.<sup>70</sup> Techniques such as grinding, thermal treatment, high-pressure lamination, and templating are instrumental in achieving this, with grinding being the primary method employed.<sup>71</sup>

Zhou's group frequently employs grinding methods to facilitate the self-assembly of POMOF materials, primarily for colourimetric or electrochemical detection of H<sub>2</sub>O<sub>2</sub> in serum. The process involves synthesising POM and MOF materials separately and then grinding and assembling them in an agate mortar in a specified ratio. This is followed by characterisation to identify POMOFs that fulfil structural criteria before delving into the study of their properties and precise synthetic steps. Notably, in the synthesis of AgFKZSiW<sub>12</sub>@PPy, a liquid phase is introduced to aid in grinding and assembly.<sup>26</sup> Despite the addition of a liquid phase, the assembly is fundamentally achieved through physical means, offering an integrated solid-phase assembly approach. The benefit of this solid-phase self-assembly strategy is its operational simplicity and broad applicability. However, challenges include difficulty in achieving precise structural and compositional control of the final product, particularly with complex hybrid materials, and potential compromises in product purity and uniformity compared to liquid-phase self-assembly.

### 3 Modification strategies

The POMOF modification strategies aim to augment the attributes of the synthesised materials *via* certain techniques to enhance their aptness and stability for targeted applications. It typically encompasses specific approaches such as ion exchange, physical adsorption, or encapsulation. Employing these techniques enables researchers to tailor POMOF materials to the exigencies of distinct applications.<sup>72</sup> This article predominantly delineates the enhancement of POMOF materials from two aspects: the amplification of catalytic efficacy and the refinement of structural integrity.

#### 3.1 Enhancement of catalytic performance

Primarily, doping synthetic composite materials serves as a means to elevate catalytic efficacy or bolster catalytic stability.<sup>73</sup> This principal approach alters the electron density and energy level distribution of POMOF materials by incorporation of distinct compounds or ions and by varying the ligand and heteroatom types. Such alterations impact the redox potential, thus enhancing electron transfer and catalytic activity. Furthermore, catalytic performance can be augmented *via* a synergistic interplay among different constituents. The maxim "the whole is greater than the sum of its parts" can be realised by integrating a cocatalyst, which steers the catalytic reaction towards a specific, precise trajectory. Modulating solubility facilitates ver-

satility across various milieus, reinforcing catalytic steadfastness.

Sha's group introduced PPy (polypyrrole) materials when preparing AgFKZSiW<sub>12</sub>@PPy<sup>26</sup> and Ag<sub>5</sub>PMo<sub>12</sub>@PPy.<sup>27</sup> As a prototypical and widely used conductive polymer, PPy is characterised by its expansive specific surface area and rapid electron transport properties. These attributes render it conducive for enhancing catalytic efficacy in conjunction with POMOF materials. Ultimately, the integration of PPy functionalisation imparts a pivotal role to POMOF materials in the detection of UA (uric acid) and AA (ascorbic acid), substantially enhancing the results' resilience against interference and yielding improved detection accuracy.

Zhou *et al.* additionally executed the functionalisation of SWCNTs (single-walled carbon nanotubes) for the synthesis of PAZ@SWCNTs-COOH.<sup>33</sup> SWCNTs boast an extensive electrochemical potential window, exceptional electrochemical traits, and biomolecule congruence. This endows them with the capacity to modulate the redox potential of the product and bolster electron transfer in catalytic reactions. Concurrently, the incorporation of SWCNTs can amplify both the mechanical robustness and biocompatibility of the product. The PAZ@SWCNTs-COOH material, derived *via* SWCNT functionalisation, demonstrated promising detection capabilities in DA (dopamine) analysis.

Incorporating compounds into POMOF materials can modify their structure to an extent, augment the exposure of active sites, and elevate catalytic performance.<sup>74</sup> Enhancing catalytic activity can refine the electronic, optical, and thermal properties of materials in line with the application context, broadening their scope of applications and enhancing the performance of functional materials. Strategies aimed at augmenting catalytic activity stand as a cornerstone in the optimisation of POMOF materials' performance.<sup>75</sup>

#### 3.2 Refinement of structure

Structural optimisation of POMOF materials constitutes a critical endeavour to enhance their performance and extend their applicability. This optimisation entails modulating POMOFs' composition, morphology, and pore architecture. The reaction enhancement is achieved by altering the morphology of POMOFs *via* structural modifications, which in turn modify their catalytic performance by adjusting the surface charge distribution and active sites.<sup>76</sup> Tailored structures predicated on application demands are engineered to enhance POMOFs' catalytic efficacy.<sup>77</sup>

Initially, reactants are gelled before the liquid-phase self-assembly of Mo-POM@HKUST-1<sup>36</sup> and NENU5-KB<sup>37</sup> materials. Pore size and distribution are tuned to yield a three-dimensional network within the POMOF, enhancing the material's adsorption capabilities. Furthermore, gelled POMOFs may exhibit improved thermal and mechanical resilience, which is crucial for specific applications. Yet, a notable drawback is the complexity of processing, with preservation posing a significant challenge.

In the synthesis of  $P_2W_{18}@Co-BTC$  for  $H_2O_2$  detection, Yu *et al.* employed a templated modification strategy.<sup>42</sup> The resulting POMOF possesses a core-shell architecture, reinforcing mechanical integrity and adsorption capacity. Subsequently, the POMOF particles are systematically affixed to a nanoscale nickel foam template, modifying the surface structure. This adjustment facilitates reactant contact with POMOFs, rendering active sites more accessible and enhancing reaction kinetics.

During the one-pot synthesis of  $CuMOFP_2W_{18}$ , Zhang *et al.* utilised a physical grinding approach to reassembling  $CuMOFP_2W_{18}$  with acetylene black (XC-72R), creating a network that encapsulates POMOFs in a relatively uniform system.<sup>35</sup> This effectively augments electron transfer within the regular network and boosts electrocatalytic performance. The spatial optimisation of POMOF materials heralds the tremendous potential for applications in sensing and detection.<sup>78</sup>

## 4 Unique properties of POMOF materials

POMOF materials, a combination of POMs and MOFs, inherit the exemplary attributes of both constituents, including the high porosity of POMs and the structural diversity of MOFs.<sup>79</sup> POMOF materials further demonstrate their unique properties. The unique properties of POMOF materials significantly enhance their applications in the biomedical field. The unique properties of POMOFs are discussed below from three aspects: the regulatability of POMOFs, stability, and their multifunctionality.

### 4.1 Regulatability

The regulatability of POMOF materials is mainly manifested in two aspects: the regulatability of catalytic activity and the regulatability of structure. In terms of catalytic activity, the type and ratio of metal centres or organic ligands in MOF materials can be customised, enabling them to exhibit a variety of enzyme-like activities, such as catalase-like (CAT-like) and peroxidase-like (POD-like) activities. Nanoscale POMs also exhibit exceptional properties in catalysing redox reactions.<sup>80</sup> POMOF materials, as a combination of both, not only integrate a variety of enzyme-like and catalytic activities but also demonstrate an enhancement in catalytic strength to a certain extent.<sup>81</sup> Ji *et al.* successfully synthesised a POMOF material by combining  $H_3PMO_{12}O_{40}$ , 3DGO, and MIL-100(Fe), exhibiting outstanding POD-like activity.<sup>31</sup> The synergistic effect of these components resulted in enhanced electrical conductivity and surface catalytic activity, surpassing that of each component. When employed for glucose (Glc) detection, this innovative material achieved a remarkably lower detection limit, and concurrently, its chemical stability was significantly improved. POMOF materials with specific catalytic properties can be tailored according to specific application environments.<sup>82</sup> The diverse and efficient catalytic characteristics of POMOFs make

them significantly valuable in the fields of anti-inflammatory and cancer therapy.

In terms of structural regulatability, based on the various preparation and modification methods mentioned above, precise control of the structure of POMOF can be achieved by altering precursors and reaction conditions. The variety of POMs, the diverse spatial structures of MOFs, and the adjustable pore size and distribution of POMOFs together provide a blueprint for the structural diversity of POMOFs. Structurally modified POMOFs demonstrate outstanding performance in drug loading, targeted drug delivery, and controlled drug release. An *et al.* created a specific structure by encapsulating  $PW_{12}$  into the UiO-67 framework, where POMs act akin to sponges, providing ample electrons to facilitate the stable adsorption of MP-11 enzymes for enzymatic therapy.<sup>51</sup> POMOFs can also be synthesised by incorporating functional groups, thus endowing the materials with specific chemical and physical properties. This enhancement facilitates interactions with specific molecules, achieves surface functionalisation, and improves the adsorption capacity for certain gases or biomolecules. Composite materials can be created by combining specific materials with POMOFs, resulting in POMOFs with distinct structural functions that exhibit excellent performance even under extreme conditions. These composite POMOF materials hold a pivotal significance in advancing sensory technology.<sup>83</sup> The potential shown by POMOFs in terms of regulatable catalytic and structural properties provides researchers with a broad scope for developing POMOFs for biomedical applications.<sup>84</sup>

### 4.2 Stability

The stability of POMOFs refers to their ability to function effectively under extreme external conditions. In the field of biomedicine, this translates to maintaining high efficiency under various biophysical conditions.<sup>85</sup> Firstly, POMOFs exhibit commendable functional stability, meaning they can maintain robust catalytic activity towards target substances even under interfering conditions. Li *et al.* combined PPy with POMOFs to form rod-like spiral structures, resulting in enhanced catalytic properties. Moreover, under the interference of factors such as Glc,  $Mg^{2+}$ ,  $Na^+$ ,  $Cl^-$ ,  $NO_3^-$ , and  $K^+$ , as well as under harsh conditions of pH and temperature, they demonstrated exceptional detection specificity for AA.<sup>26</sup> Secondly, there is structural stability, where under biomedical conditions, POMOFs can maintain their porous structure largely intact. Although POMOFs tend to aggregate under physiological conditions, this effect can be mitigated to a certain extent through modification and regulation. Liu *et al.* synthesised W-POM NCs@HKUST-1 for combined chemodynamic therapy (CDT) and photothermal therapy (PTT).<sup>46</sup> The resultant encapsulated structure exhibited good dispersibility in RPMI-1640 aqueous cell culture medium containing fetal bovine serum for seven days, with no significant macroscopic aggregation observed. This can be attributed, to a certain extent, to the synergistic effect of gallic acid and the charge effect stability of HKUST-1, which enhances the structural stability of POMOFs. The com-



combined stability of catalytic performance and structure lays a foundation for the application of POMOFs in the field of biomedicine.

### 4.3 Multifunctionality

In addition to their exceptional regulatability and good stability, POMOFs also possess multifunctional characteristics. POMs, known for their photothermal effects, are commonly used in PTT. MOFs, while providing a stable framework, also introduce various enzyme-like activities, endowing POMOFs with excellent CDT characteristics in the biomedical field.<sup>86</sup> Consequently, POMOF materials exhibit multifunctional features by enabling simultaneous multiple therapeutic approaches. Liu and colleagues synthesised W-POM NCs@HKUST-1 materials, under NIR light irradiation, and combined photothermal therapy with dynamic therapy, producing a synergistic treatment effect on tumour cells.<sup>46</sup> Our group synthesised POM@ZIF-8 NPs, combining electrocatalytic and dynamic properties to conduct Electrodynamical therapy (EDT) and CDT.<sup>47</sup> The functional diversity of POMOFs offers broad prospects for material development, making it an exciting area of research in the field of biomedicine.<sup>87</sup>

## 5 Biomedical applications

POMOFs, as popular materials in recent years, have a wide range of applications in the biomedical field. The main mechanism of action is that POMOFs have good POD-like, electrochemical catalytic activity, and good adsorption properties. At the same time, POMOF materials have good biocompatibility and can be used in the biomedical detection field as potential materials for supercapacitors. Its potential catalytic activity also enables its application in the field of biomedical therapy. The following focuses on the biomedical applications of POMOF materials from two aspects: biodetectors and biomedical therapies.

### 5.1 Biosensors

POMOF materials have POD-like and electrochemical catalytic activities for different substrate reactions. Due to the perfect performance of these activities, POMOF materials can be used for applications in the field of biosensors.<sup>88</sup> POMOF materials biosensors have the advantages of high selectivity against interference and low detection limits. Their biocompatibility and nature as a promising material for supercapacitors allow them to be used for colourimetric and electrochemical detections, and the application of POMOF materials to the sensing of physical quantities and the detection of different substrates by these two methods is presented below. Table 2 demonstrates the linear detection range and LOD (limit of detection) of POMOF biosensors.

**5.1.1 Colourimetric biosensors.** The colourimetric method is a method to determine the content of the components of the substance to be measured by comparing or measuring the depth of the colour change of the coloured substance solu-

tion.<sup>89</sup> In addition, the colour change of the excitation spectrum of the effective component adsorbed in POMOFs can be caused by the change in some physical quantities. The colourimetric method has the advantages of simple operation, a wide range of uses, low cost, *etc.* It is often widely used.<sup>90</sup> The colourimetric method can be divided into the visual colourimetric method, and the photoelectric colourimetric method, and the photoelectric colourimetric method is often used in biological or medical fields.<sup>91</sup> POMOF materials for substrate colourimetric detection mechanism: often through the reaction of substrate by-products and colour source reagents to react and then detect the change in colour absorbance to determine the concentration of the substrate, this reaction is usually based on H<sub>2</sub>O<sub>2</sub>-mediated reaction, colour source reagents are usually selected TMB (3,3',5,5'-tetramethylbenzidine) and so on. The POMOF materials colourimetric detector includes the following two presentations: 1 colour change of the system due to changes in the physical properties of the system. This paper is about sensing pH and temperature. 2 Quantitative detection of the target substance by detecting changes in colour absorbance.

**5.1.1.1 pH sensing.** pH is an important scale for indicating the strength of acids and bases and has been used in a wide variety of scientific applications since its introduction. It plays a vital role in the design of batteries, in the field of food, and in the diagnosis and treatment of diseases.<sup>92</sup> The level of pH in the body is also an essential gauge of the abnormalities of the internal environment of human tissues.<sup>93</sup> Currently, pH test strips and pH meter methods are the main methods for detecting pH.<sup>94</sup> The redox potential of POMOF materials is highly sensitive to pH and can be used as a potentiometric pH sensor.

Wang *et al.* synthesised the {Mn(3-dpye)<sub>0.5</sub>[CrMo<sub>6</sub>(OH)<sub>6</sub>O<sub>18</sub>](H<sub>2</sub>O)}·(3H<sub>2</sub>dpye)<sub>0.5</sub> (3-dpye = *N,N'*-bis(3-pyridinecarboxamide)-1,2-ethane) by using one-pot method can be used for sensing of pH detection.<sup>21</sup> The detection mechanism was that the POMOFs material modified electrode was used for the electrochemical detection of pH and showed redox activity by cyclic voltammetry scanning to know that pH was correlated with electrochemical behaviour and showed an electrochemical response. Therefore, POMOF materials can make sensor material as a potentiometric pH sensor and exhibit high sensitivity and interference resistance.

**5.1.1.2 Temperature sensing.** Temperature is a physical quantity that indicates the degree of heat or cold of an object and is an important indicator in industry, agriculture, and medicine.<sup>95</sup> In the field of biomedicine, low body temperature not only represents a system disorder but also causes cardiovascular and cerebrovascular diseases. At the same time, high body temperature can also cause abnormalities in the function of the body's internal organs, so temperature detection is also an important area of biosensing.<sup>96</sup> The POMOF materials also provide a colourimetric method for temperature detection.

Kaczmarek synthesised POM@MOF doped with Eu<sup>3+</sup> and Tb<sup>3+</sup>, whose emission light colour changes significantly with temperature.<sup>22</sup> The principle is the excitation spectrum of Eu.



**Table 2** The linear detection range and LOD of POMOFs biosensors

Applications	Abbreviations	Linear range	LOD
H <sub>2</sub> O <sub>2</sub>	CuSiW <sub>12</sub>	1–60 μM	0.10 μM
L-Cysteine	Cu <sub>18</sub> PW <sub>12</sub> /SWNTs	1–80 μM	0.103 mM
AA&H <sub>2</sub> O <sub>2</sub>	AgFKZSiW <sub>12</sub> @PPy	1–80 μM AA 1–100 μM H <sub>2</sub> O <sub>2</sub>	2.7 μM AA 0.12 μM H <sub>2</sub> O <sub>2</sub>
UA	Ag <sub>5</sub> PMO <sub>12</sub> @PPy	1–50 μM	0.47 μM
AA&H <sub>2</sub> O <sub>2</sub>	CuFKZP <sub>2</sub> W <sub>18</sub> /PPy	5–10 μM AA 5–100 μM H <sub>2</sub> O <sub>2</sub>	0.627 μM AA 0.72 μM H <sub>2</sub> O <sub>2</sub>
CA&H <sub>2</sub> O <sub>2</sub>	Ni <sub>4</sub> SiW <sub>12</sub> /PDDA-rGO	1–60 μM CA 1–100 μM H <sub>2</sub> O <sub>2</sub>	2.07 μM AA 0.49 μM H <sub>2</sub> O <sub>2</sub>
L-Cysteine	NiMo <sub>6</sub> @ZIF-67	1–20 μM	0.018 μM
Glc	MIL-100@PMO <sub>12</sub>	1–100 μM	0.14 μM
Glc	MIL-101@P <sub>2</sub> W <sub>18</sub>	1–150 μM	0.2 μM
DA	PAZ@SWCNTs-COOH	0.05–100 μM	8.6 nM
DA	V <sub>10</sub> O <sub>28</sub> @NU-902	25–400 μM	2.1 μM
XA	CuMOFP <sub>2</sub> W <sub>18</sub>	0.5–240 μM	0.26 μM
L-Cysteine	Mo-POM@HKUST-1	3–10 mM	0.307 μM
H <sub>2</sub> O <sub>2</sub>	NENU5-KB	10–50 mM	1.03 μM
H <sub>2</sub> O <sub>2</sub>	AsW <sub>12</sub> @MOF	1.43–1890 μM	0.48 μM
H <sub>2</sub> O <sub>2</sub>	Ag <sub>5</sub> [BW <sub>12</sub> O <sub>40</sub> ]@Ag-BTC-2	0.4–270 μM	0.19 μM
H <sub>2</sub> O <sub>2</sub>	Co <sub>3</sub> Mo <sub>7</sub> O <sub>24</sub> @Ag-BTC-2	1–430 μM	0.33 μM
H <sub>2</sub> O <sub>2</sub>	Ag <sub>4</sub> K <sub>2</sub> P <sub>2</sub> W <sub>18</sub> O <sub>62</sub> @Ag-BTC-7	1.5–1500 μM	0.206 μM
H <sub>2</sub> O <sub>2</sub>	P <sub>2</sub> W <sub>18</sub> @Co-BTC	1.9–1670 μM	0.633 μM
H <sub>2</sub> O <sub>2</sub>	[Ag <sub>5</sub> (pz) <sub>6</sub> (H <sub>2</sub> O) <sub>4</sub> ][BW <sub>12</sub> O <sub>40</sub> ]	5–270 μM	2.2 μM
H <sub>2</sub> O <sub>2</sub>	Ni <sub>3</sub> P <sub>2</sub> W <sub>18</sub> O <sub>62</sub> -Ni <sub>3</sub> (BTC) <sub>2</sub>	0.5–250 μM	0.17 μM
H <sub>2</sub> O <sub>2</sub>	HRBNU-7	0.5–300 μM	0.17 μM

The temperature is related to the frequency of the excitation spectrum. When the temperature increases the emission colour of the compound from blue-violet (60 K) to orange (360 K), POMOF materials effectively increase the sensitivity of temperature detection. The method shows a good detection width of 60–360 K and 0.71% K<sup>-1</sup> sensitivity, so POMOF materials can be used to make sensor material used as a colourimetric temperature sensor.

Viravaux *et al.* similarly synthesised POMOF materials doped with 9.1 wt% and 19.5 wt% EuW<sub>10</sub>@Tb-TATB-DMA (TATB = 1,3,5-triamino-2,4,6-trinitrobenzenet, DMA = dimethylacetamide), which can be used for the detection of temperature.<sup>23</sup> The principle is also the excitation spectrum of Eu, where the temperature is related to the frequency of the excitation spectrum and exhibits good thermal sensitivity. This method displays a good detection width of 200–320 K, 9.1 wt% EuW<sub>10</sub>@Tb-TATB Showing a sensitivity of 2.68% K<sup>-1</sup>, 19.5 wt% EuW<sub>10</sub>@Tb-TATB Showing a sensitivity of 2.37% K<sup>-1</sup>.

**5.1.1.3 Detection of substrates.** Jingquan Sha's group has made significant contributions in the field of colourimetric detection of POMOF materials, and their work is summarised and reviewed in chronological order below.

Li *et al.* synthesised the POMOF materials [Cu<sub>5</sub>(pz)<sub>6</sub>Cl][SiW<sub>12</sub>O<sub>40</sub>] (pz = pyrazine) for the colourimetric detection of H<sub>2</sub>O<sub>2</sub>.<sup>24</sup> The detection mechanism is CuSiW<sub>12</sub> exerting POD-like enzyme activity and then producing the colour change with TMB colour source reagent, which can be used for the quantitative determination of H<sub>2</sub>O<sub>2</sub> by detecting absorbance into the standard curve. The same method is used to determine the H<sub>2</sub>O<sub>2</sub> content by measuring the absorbance of the unknown sample after the standard curve is made. The

linear detection limit of H<sub>2</sub>O<sub>2</sub> is 1–60 μM, and the LOD is 0.10 μM.

Li *et al.* synthesised POMOF materials by one-pot method for the colourimetric detection of AA and H<sub>2</sub>O<sub>2</sub>.<sup>26</sup> The POMOF materials were first synthesised by the one-pot method of [Ag<sub>3</sub>(FKZ)<sub>2</sub>(H<sub>2</sub>O)<sub>2</sub>][H<sub>3</sub>SiW<sub>12</sub>O<sub>40</sub>] (HKZ = 1-(2,4-difluorophenyl)-1,1-bis[(1H-1,2,4-triazol-1-yl)methyl] ethanol) of POMOF materials. Then, the surface structure of the POMOF material was modified to get the AgFKZSiW<sub>12</sub>@PPy composites for detection. The detection mechanism is that AgFKZSiW<sub>12</sub>@PPy exerts POD-like enzyme activity on AA and H<sub>2</sub>O<sub>2</sub> and later produces colour change with TMB colour source reagent, which can be used for quantitative detection of AA and H<sub>2</sub>O<sub>2</sub> by detecting absorbance. The detection was performed by making standard absorbance curves for AA and H<sub>2</sub>O<sub>2</sub> in the presence of acetate buffer and then measuring the absorbance of unknown samples under the same conditions to determine the unknown concentration of AA and H<sub>2</sub>O<sub>2</sub> solutions. The linear detection limit of AA was 1–80 μM with a LOD of 2.7 μM. The linear detection limit of H<sub>2</sub>O<sub>2</sub> was 1–100 μM with a LOD of 0.12 μM.

Li *et al.* also synthesised Nano-POMOF materials [Cu<sub>18</sub>(trz)<sub>12</sub>Cl<sub>3</sub>(H<sub>2</sub>O)<sub>2</sub>][PW<sub>12</sub>O<sub>40</sub>] (trz = 1,2,4-triazole) by ultrasonic drive self-assembly strategy and then combined with SWNTs by ultrasonic centrifugation to form Cu<sub>18</sub>PW<sub>12</sub>NC/SWNTs composites for colourimetric detection of L-cysteine.<sup>25</sup> The detection mechanism is that Cu<sub>18</sub>PW<sub>12</sub>NC/SWNTs can exert a specific POD-like enzymatic activity on L-cysteine and later produce a colour change with TMB chromogenic reagent, which can be used for the quantitative detection of L-cysteine by detecting the absorbance. Fig. 2 presents the detailed absor-

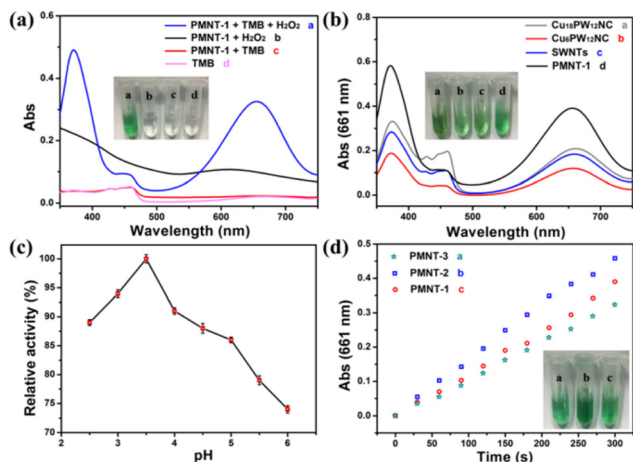


**Fig. 2** Applications of the  $\text{Cu}_{18}\text{PW}_{12}\text{NC}/\text{SWNTs}$  in the detection of L-cysteine. (a) UV-vis absorbance curves of the different reaction systems (pH = 3.5, 40 °C, 5 min). (b) UV-vis absorbance curves and the pertinent photographs of absorption mode with different catalysts. (c) The relationship of the POD-like activity of  $\text{Cu}_{18}\text{PW}_{12}\text{NC}/\text{SWNTs}$  with different pH values. (d) UV-vis absorption maps and related photographs of  $\text{Cu}_{18}\text{PW}_{12}\text{NC}/\text{SWNTs}$  with different ratios in the presence of fixed TMB (150  $\mu\text{M}$ ) and  $\text{H}_2\text{O}_2$  (100  $\mu\text{M}$ ).<sup>25</sup> Copyright 2019, American Chemical Society.

bance standard curve for colourimetry alongside a comparative graph. The linear detection limit of the method is 1–80  $\mu\text{M}$ , and the LOD is 0.103 mM.

A colourimetric detection for UA without uricase was also developed by the one-pot method.<sup>27</sup> The research group synthesised  $\text{Ag}_5[\text{bimt}]_2[\text{PMo}_{12}\text{O}_{40}] \cdot 2\text{H}_2\text{O}$  ( $\text{Ag}_5\text{PMo}_{12}$ ) (Hbimt = 3,5-bis((1*H*-imidazol-1-yl)methyl)-1*H*-1,2,4-triazole) by one-pot method and synthesised  $\text{Ag}_5\text{PMo}_{12}@\text{PPy}$  composite for colourimetric detection of UA by precipitation method for modification of POMOF materials. The detection mechanism (Fig. 3):  $\text{Ag}_5\text{PMo}_{12}@\text{PPy}$  exerted POD-like activity carried out by  $\text{H}_2\text{O}_2$ -mediated TMB colour source reagent to produce a colour change. The detection method: a standard absorbance curve is developed through the reaction of a standard uric acid solution. The concentration of an unknown sample of a certain concentration can be obtained by detecting the absorbance. The detection demonstrates excellent selectivity and reproducibility for UA detection under the interference of AA, urea, triglyceride, cholesterol, grape, and other metal ions. The linear detection limit was 1–50  $\mu\text{M}$ , and the LOD was 0.47  $\mu\text{M}$ .

Li *et al.* synthesised Wells–Dawson-type POMOF material  $\text{CuFKZP}_2\text{W}_{18}/\text{PPy}$  by one-pot method for the colourimetric detection of AA and  $\text{H}_2\text{O}_2$ .<sup>28</sup> Through the incorporation of PPy as a modification agent, a profound alteration is instilled within the electrochemical activity of the POMOFs. This transformative intervention engenders an expansion of its reaction contact area, thereby conferring a distinct advantage to the POMOFs in realising an enhanced catalytic performance. The detection mechanism is that  $\text{CuFKZP}_2\text{W}_{18}/\text{PPy}$  exerts high POD-like activity and electrochemical activity on AA and  $\text{H}_2\text{O}_2$ .

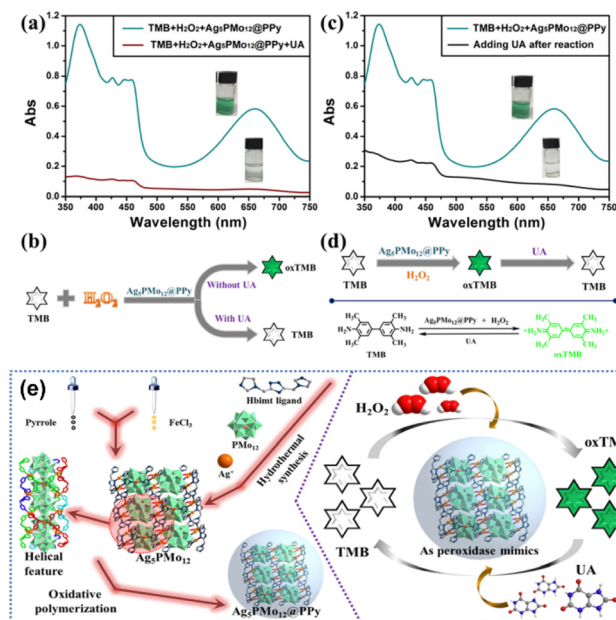


**Fig. 3** Applications of the  $\text{Ag}_5\text{PMo}_{12}@\text{PPy}$  in the detection of UA. (a) Absorption spectra of the  $\text{Ag}_5\text{PMo}_{12}@\text{PPy}$  system with or without UA after the reaction. (b) Schematic illustration of the reaction. (c) Absorption spectra of the  $\text{Ag}_5\text{PMo}_{12}@\text{PPy}$  system with or without UA after the reaction. (d) Schematic illustration of the corresponding process. (e) Schematic illustration of the synthesis of  $\text{Ag}_5\text{PMo}_{12}@\text{PPy}$  and the corresponding colourimetric UA biosensor.<sup>27</sup> Copyright 2020, American Chemical Society.

The detection method is similar to the above assay. The linear detection limit was 5–100  $\mu\text{M}$  for AA with a LOD of 0.627  $\mu\text{M}$ .

A biological colourimetric method for the determination of CA (citric acid) and  $\text{H}_2\text{O}_2$  was first designed by Sha *et al.*<sup>29</sup> POMOF material was synthesised by firstly synthesising MOF framework  $\text{Ni}_4\text{SiW}_{12}$  by one-pot method, and then one-pot self-assembled with PDDA-rGO (poly (diallyldimethylammonium chloride) functionalised reduced graphene oxide) to synthesise  $\text{Ni}_4\text{SiW}_{12}/\text{PDDA-rGO}$  for detection of CA and  $\text{H}_2\text{O}_2$ . Its detection mechanism (Fig. 4) is that PMPG-*n* catalyses the decomposition of  $\text{H}_2\text{O}_2$  with POD-like activity and then reacts with chromogenic reagent TMB to change the colour. The system changes from colourless to green, and the system changes from green to colourless after adding CA. The detection procedure is as follows: add POMOF, TMB,  $\text{H}_2\text{O}_2$ , and an unknown concentration of CA in acetate buffer solution at pH = 2.5, filter and transfer to a quartz test tube, and detect the concentration of CA and  $\text{H}_2\text{O}_2$  by using UV-Vis spectrophotometer to detect the absorbance change of the system into the standard curve. The linear range of CA was from 1–60  $\mu\text{M}$  with a LOD of 2.07  $\mu\text{M}$ . The linear range of  $\text{H}_2\text{O}_2$  was from 1–100  $\mu\text{M}$  with a LOD of 0.49  $\mu\text{M}$ , and the POMOF materials showed high interference resistance for both substrates.

Ji *et al.* crafted  $\text{MIL-100}(\text{Fe})@\text{PMo}_{12}@3\text{DGO}$  for the colourimetric detection of Glc.<sup>31</sup> This composite was engineered by encasing Keggin-type  $\text{H}_3\text{PMo}_{12}\text{O}_{40}$  within the MIL-100

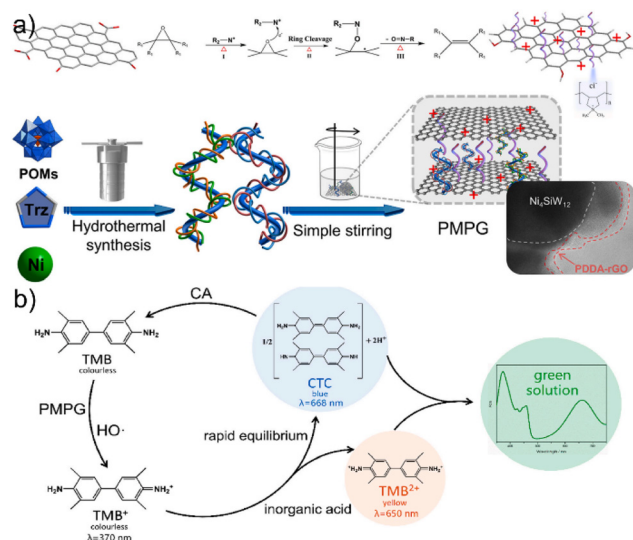


**Fig. 4** Applications of the  $\text{Ni}_4\text{SiW}_{12}/\text{PDDA-rGO}$  in the detection of CA. (a) Schematic illustration of synthesizing  $\text{Ni}_4\text{SiW}_{12}/\text{PDDA-rGO}$ . (b) Schematic illustration of detecting CA using  $\text{Ni}_4\text{SiW}_{12}/\text{PDDA-rGO}$ .<sup>29</sup> Copyright 2020, Elsevier.

scaffold, followed by a coating with three-dimensional graphene (3DGO) to enhance conductivity, surface area, porosity, and chemical robustness. The resulting nanocomposite exhibited superior POD-like activity and provided a linear detection scope from 1 to 100  $\mu\text{M}$ , achieving a low Glc detection LOD of 0.14  $\mu\text{M}$ .

The researcher synthesised and assembled porous  $\text{NiMo}_6@\text{Co}_3\text{O}_4$  materials for the detection of L-cysteine by the colourimetric method.<sup>30</sup> The detection mechanism (Fig. 5) is that  $\text{NiMo}_6@\text{ZIF-67}$  can play a certain POD-like enzyme activity on L-cysteine for the  $\text{H}_2\text{O}_2$ -mediated L-cysteine reaction and the reaction produces a colour change with TMB, which can be used for the quantitative detection of L-cysteine by detecting the absorbance. The detection is based on the POMOF-catalyzed L-cysteine action followed by  $\text{H}_2\text{O}_2$ -mediated binding action with TMB for absorbance detection to obtain the L-cysteine content. The linear detection limit of L-cysteine was 1–20  $\mu\text{M}$ , and the LOD was 0.018  $\mu\text{M}$ .

Liu *et al.* fabricated  $\text{MIL-101}(\text{Fe})@\text{P}_2\text{W}_{18}@\text{SWNT}$  for the colourimetric detection of  $\text{H}_2\text{O}_2$  and Glc.<sup>32</sup> This nanocomposite

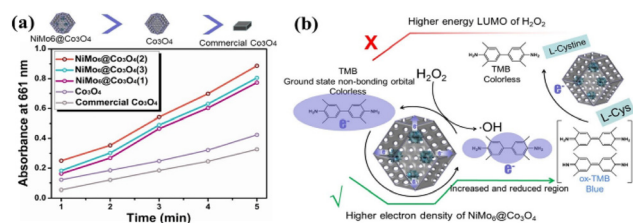


**Fig. 5** Applications of the  $\text{NiMo}_6@\text{Co}_3\text{O}_4$  in the detection of L-cysteine. (a) The absorbance changes at 661 nm of  $\text{NiMo}_6@\text{Co}_3\text{O}_4$ ,  $\text{Co}_3\text{O}_4$ , and commercial  $\text{Co}_3\text{O}_4$ . (b) Schematic illustration of biosensing L-cysteine.<sup>30</sup> Copyright 2021, John Wiley and Sons.

exhibits superior peroxidase-mimicking properties and stability thanks to the collective and optimally synergistic effects of its components. Fig. 6 shows the specific characterisation and detection standard curve of  $\text{MIL-101}(\text{Fe})@\text{P}_2\text{W}_{18}@\text{SWNT}$ . Leveraging the remarkable catalytic prowess of  $\text{MIL-101}(\text{Fe})@\text{P}_2\text{W}_{18}@\text{SWNT}$ , dual colourimetric biosensors were developed to detect  $\text{H}_2\text{O}_2$  and Glc, achieving linear detection ranges of 0–80  $\mu\text{M}$  ( $\text{H}_2\text{O}_2$ ) and 0–150  $\mu\text{M}$  (Glc), with detection limits of 0.3  $\mu\text{M}$  ( $\text{H}_2\text{O}_2$ ) and 0.2  $\mu\text{M}$  (Glc), respectively.

**5.1.2 Electrochemical biosensors.** The electrochemical detection method is based on the electrochemical properties of the substances in solution and their change regulation.<sup>97</sup> The electrochemical detection method is based on the qualitative and quantitative analysis of components based on the stoichiometric relationship between electrical quantities such as potential, conductance, current, and electricity and certain quantities of the measured substance.<sup>98</sup> The electrochemical detection methods contain conductivity methods, potentiometric titration, electrolytic analysis, voltammetry, dissolution voltammetry, and coulometric analysis.<sup>99</sup> The electrochemical detection method has the advantages of high sensitivity, high accuracy, and wide measurement range and is widely used for electrochemical testing of POMOF material applications.<sup>100</sup> The following are electrochemical detection applications for POMOF materials.

Zhou *et al.* used DPV (differential pulse voltammetry) to conduct electrochemical detection of DA through modified POMOF materials.<sup>33</sup> The POMOF material of  $[\text{Ag}_5(\text{trz})_4]_2\text{[PMO}_{12}\text{O}_{40}]$  (PAZ) was synthesised by the one-pot method, and then the POMOF material was modified by adding new compounds to make the composite modified electrode of  $\text{PAZ}@\text{SWCNTs-COOH}/\text{GCE}$ . The detection mechanism is that the  $\text{PAZ}@\text{SWCNTs-COOH}/\text{GCE}$  material exerts electrochemical activity with DA, producing potential changes that can be used for DPV detection.<sup>101</sup> The detection was performed by sequentially dispersing the PAZ solution into deionised water to obtain a suspension. The quantitative determination of DA in serum is performed by DPV. The pulse amplitude, pulse width, pulse period, and amplitude are selected after the pretreatment of human serum samples. The linear range of the DA was 0.05–100  $\mu\text{M}$  with a LOD of 8.6 nM.

Ho *et al.* prepared  $\text{V}_{10}\text{O}_{28}@\text{NU-902}$  as a non-homogeneous electrocatalyst for electrochemical DA sensors by impregnation method.<sup>34</sup> The detection mechanism is that  $\text{V}_{10}\text{O}_{28}@\text{NU-902}$  exerts redox activity with dopamine, producing potential changes that can be used for cyclic voltammetry detection. The detection was performed by placing the  $\text{V}_{10}\text{O}_{28}@\text{NU-902}$  non-homogeneous electrocatalyst film in an electrolyte. The method has a linear detection range of 25–400  $\mu\text{M}$  for DA and a LOD of 2.1  $\mu\text{M}$ .

Zhang *et al.* provided a method for the cyclic voltammetry detection of XA (xanthine) in POMOF materials.<sup>35</sup> The MOF framework of  $\text{CuMOFP}_2\text{W}_{18}$  was synthesised by the one-pot method, and then the POMOF material of  $\text{CuMOFP}_2\text{W}_{18}/\text{XC-72R}/\text{GCE}$  ( $\text{XC-72R}$  = acetylene black) was self-assembled by grinding and sonication. The detection mechanism was that



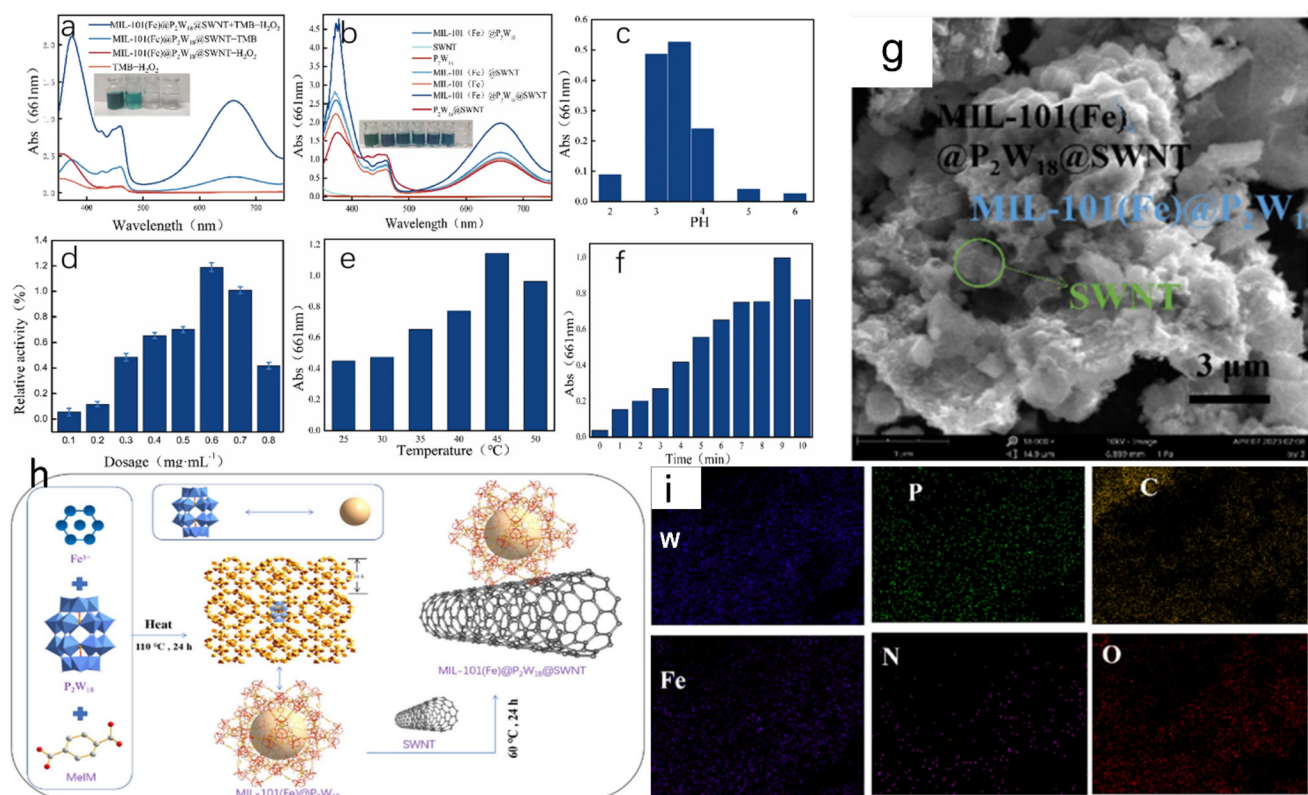


**Fig. 6** Applications of the MIL-101(Fe)@P<sub>2</sub>W<sub>18</sub>@SWNT in the detection of H<sub>2</sub>O<sub>2</sub> and Glc. (a) UV-vis absorbance curves of MIL-101(Fe)@P<sub>2</sub>W<sub>18</sub>@SWNT + H<sub>2</sub>O<sub>2</sub> + TMB, MIL-101(Fe)@P<sub>2</sub>W<sub>18</sub>@SWNT + H<sub>2</sub>O<sub>2</sub>, MIL-101(Fe)@P<sub>2</sub>W<sub>18</sub>@SWNT + TMB, H<sub>2</sub>O<sub>2</sub> + TMB. (b) UV-vis absorbance curves of different MIL-101(Fe)@P<sub>2</sub>W<sub>18</sub>@SWNT systems (pH = 3.5, 100 μM H<sub>2</sub>O<sub>2</sub>, 0.6 mg mL<sup>-1</sup> catalyst, 0.5 mM TMB, at 45 °C for 9 min). Dependence of the POD-like activity on (c) pH. (d) MIL-101(Fe)@P<sub>2</sub>W<sub>18</sub>@SWNT dosage. (e) Temperature. (f) Time. (g) SEM images of MIL-101(Fe)@P<sub>2</sub>W<sub>18</sub>@SWNT. (h) Schematic illustration of the synthesis routes of ternary MIL-101(Fe)@P<sub>2</sub>W<sub>18</sub>@SWNT. (i) Elemental mapping images of MIL-101(Fe)@P<sub>2</sub>W<sub>18</sub>@SWNT.<sup>32</sup> Copyright 2023, Springer Nature.

the POMOF materials exerted significant electrocatalytic activity to promote XA oxidation. The detection mechanism is that different volumes of standard XA solutions were added to diluted human serum samples. After each addition, voltammograms were recorded over a range of potentials, peak currents were estimated, calibration curves were calibrated based on the standard samples, and the concentration of XA in the serum samples was calculated. The linearity range was 0.5–240 μM, with a LOD of 0.26 μM and good selectivity, and stability.

A method for the cyclic voltammetry detection of L-cysteine in POMOF materials was provided by Murinzi *et al.*<sup>36</sup> The process involved the synthesis of the MOF framework HKUST-1 *via* one-pot methods, followed by further modification with Mo-POM using a one-pot technique. Subsequently, the modified Mo-POM was integrated onto a doped Mo-POM-GCE electrode to enable electrochemical detection of L-cysteine. The mechanism of detection relied on the electrochemical catalytic activity of Mo-POM towards L-cysteine, with alterations in its potential being quantified *via* cyclic voltammetry. A standard curve was generated utilising concentrations of known samples, allowing for the analysis of unknown

samples. The assay demonstrated a linear detection range of 3–10 mM and a LOD of 0.307 μM.

Wang *et al.* provided an enzyme-free method for detecting H<sub>2</sub>O<sub>2</sub> by POMOF.<sup>37</sup> This approach presents a novel enzyme-free concept for catalysing reactions and their application in detection. As the field of nanozyme research continues to advance, the potential synergy between POMOF materials and nanozymes could lead to significant advancements in enzyme-free detection methodologies. The POMOF materials were synthesised by first synthesizing [Cu<sub>2</sub>(BTC)<sub>4</sub>(H<sub>2</sub>O)<sub>2</sub>]<sub>6</sub> [H<sub>3</sub>PMo<sub>12</sub>O<sub>40</sub>] (NENU5) (H<sub>3</sub>BTC = 1,3,5-benzenetricarboxylic acid), by a solvothermal method, and NENU5-KB materials were synthesised by applying compounds modification with KB (ketjenblack). The detection mechanism is that the POMOF material exhibits a unique redox activity that can act as an efficient electrochemical activity to promote H<sub>2</sub>O<sub>2</sub> decomposition, and H<sub>2</sub>O<sub>2</sub> was detected using cyclic voltammetry analysis. The detection method is the prepared NENU5-KB material-modified GC electrode for cyclic voltammetry detection of standard H<sub>2</sub>O<sub>2</sub> solution to make a standard curve and then measure the unknown sample potential to get the unknown H<sub>2</sub>O<sub>2</sub> concentration (Fig. 7). This method has a

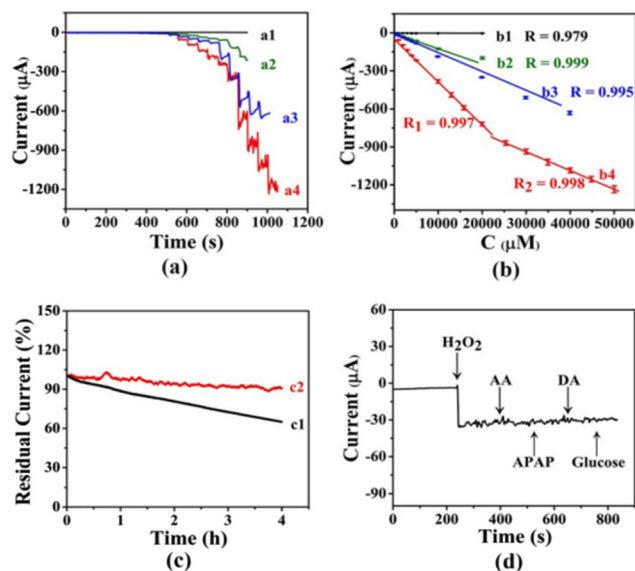


**Fig. 7** Applications of the NENU5-KB in the detection of L-cysteine. (a) Amperometric current-time curves of different systems with the addition of  $\text{H}_2\text{O}_2$  (system 1 = GCE, system 2 = HKUST-1/GCE, system 3 = HKUST-1-KB-3/GCE, and system 4 = NENU5-KB-3/GCE). (b) Current curves of different systems with the addition of  $\text{H}_2\text{O}_2$ . (c) Stability of current response of systems 1 and 2. (d) Current-time curve of system 4 with the addition of 0.5 mM  $\text{H}_2\text{O}_2$ , 0.2 mM AA, 0.2 mM APAP (acetaminophen), 0.2 mM DA, and 0.2 mM Glc. The electrolyte in systems 1, 3, and 4 was  $\text{N}_2$ -saturated 0.1 M PBS (pH = 7.4). The applied potential in systems 1, 3, and 4 was 0.47 V.<sup>37</sup> Copyright 2018, John Wiley and Sons.

linear detection range of 10–50 mM for  $\text{H}_2\text{O}_2$ , with a LOD of 1.03  $\mu\text{M}$ , and exhibits high sensitivity.

Baibin Zhou's group has made significant contributions to the field of electrochemical biosensors of POMOF materials, and their related work is summarised and reviewed in chronological order below.

Cui *et al.* proposed a method for grafted POMOF to detect  $\text{H}_2\text{O}_2$  by cyclic voltammetry and chronoamperometry.<sup>38</sup> The POMOF material synthesis method is to synthesise ( $\text{AsW}_{12}\text{@MOF}$ ) [ $(\text{Ag}(\text{bpy})_2\text{Cl}_2)\{\text{As}(\text{W}^{\text{VI}})_2(\text{W}^{\text{VI}})_{10}\text{O}_{40}\}\cdot\text{H}_2\text{O}$ ] (bpy = 4,4'-bipyridyl) on MOF by solid-phase self-assembly method. The detection mechanism is the catalytic redox activity of the POMOF material for  $\text{H}_2\text{O}_2$ . The detection method is to make an  $\text{AsW}_{12}\text{@MOF-GCE}$  electrode to detect  $\text{H}_2\text{O}_2$ .  $\text{AsW}_{12}\text{@MOF-GCE}$  electrode for cyclic voltammetry detection of  $\text{H}_2\text{O}_2$ . Construct the standard curve by plotting the concentrations of the known samples and subsequently analyse the unknown sample.  $\text{H}_2\text{O}_2$  was detected linearly in the range of 1.43–1890  $\mu\text{M}$  with a LOD of 0.48  $\mu\text{M}$ .

Yu *et al.* also provided a method for cyclic voltammetry detection of  $\text{H}_2\text{O}_2$  by core-shell POMOF.<sup>39</sup> POMOF material synthesis method  $\text{Ag}_5[\text{BW}_{12}\text{O}_{40}]$  was synthesised by mixing  $\text{AgNO}_3$  with  $\text{K}_5[\text{BW}_{12}\text{O}_{40}]\cdot 15\text{H}_2\text{O}$ . Then  $\text{Ag}_5[\text{BW}_{12}\text{O}_{40}]$  and Ag-BTC were ground in a mortar to synthesise  $\text{Ag}_5[\text{BW}_{12}\text{O}_{40}]\text{@Ag-BTC-2}$ . The catalytic mechanism is the highly potent redox activity of POMOF by the action of  $\text{H}_2\text{O}_2$ , with a linear detection range of 0.4–270  $\mu\text{M}$  for  $\text{H}_2\text{O}_2$  and a LOD of 0.19  $\mu\text{M}$ .

Yu *et al.* provided a method for detecting  $\text{H}_2\text{O}_2$  by chronoamperometry and cyclic voltammetry for POMOF materials.<sup>40</sup> The POMOF material synthesis method was modified and synthesised by solid-phase self-assembly method with  $\text{Co}_3\text{Mo}_7\text{O}_{24}\text{@Ag-BTC-2}$ , and the POM material was injected into MOFs. The detection mechanism is electrochemical catalysis of  $\text{H}_2\text{O}_2$ , and the response current is gradually enhanced with increasing  $\text{H}_2\text{O}_2$  concentration in electrochemical characterisation. The detection process: using the material as the working electrode, using the platinum sheet as the counter electrode, using the saturated calomel electrode as the reference electrode, using the chronoamperometry and cyclic voltammetry calibration, detecting the unknown sample potential to obtain the unknown sample concentration. The linear detection range of  $\text{H}_2\text{O}_2$  is 1–430  $\mu\text{M}$ , and the LOD is 0.33  $\mu\text{M}$ .

Liang *et al.* provided a method for cyclic voltammetry detection of  $\text{H}_2\text{O}_2$  in POMOFs ( $\text{Ag}_4\text{K}_2\text{P}_2\text{W}_{18}\text{O}_{62}\text{@Ag-BTC-}n$ ).<sup>41</sup> POMOFs material was synthesised through a liquid-assisted grinding method, with a coating structure designed to increase surface area and electron transfer efficiency. Its detection mechanism is that  $\text{Ag}_4\text{K}_2\text{P}_2\text{W}_{18}\text{O}_{62}\text{@Ag-BTC-}n$  assembly enhances the catalytic play of the electrochemically active role of  $\text{H}_2\text{O}_2$ , and it can play electrocatalytic activity. Based on this electrocatalytic activity, there is a certain mathematical relationship between current and voltage. The response current is gradually improved with increasing  $\text{H}_2\text{O}_2$  concentration in electrochemical characterisation. Fig. 8 shows some characterisation and electrochemical detection of POMOF materials in this case. The linear range of  $\text{H}_2\text{O}_2$  detection was 1.5–1500  $\mu\text{M}$ , and the LOD was 0.206  $\mu\text{M}$  with a high recovery of 97.54–99.61%.

The symmetrical two-electrode system made of Dawson-type POMOF materials also provided a method for detecting  $\text{H}_2\text{O}_2$ .<sup>42</sup> POMOF materials are synthesised by hydrothermal synthesis of MOF materials followed by solid phase grinding method to combine POM and MOF to synthesise  $\text{CoK}_4[\text{P}_2\text{W}_{18}\text{O}_{62}]\text{@Co}_3(\text{btc})_2$  material. The detection mechanism is to make  $\text{CoK}_4[\text{P}_2\text{W}_{18}\text{O}_{62}]\text{@Co-BTC-GCE}$  electrode to make a CV curve. POMOF material has strong redox activity and electrochemical activity of  $\text{H}_2\text{O}_2$ , the response is current and  $\text{H}_2\text{O}_2$  concentration to make the standard curve. The concentration of  $\text{H}_2\text{O}_2$  in the unknown serum can then be obtained from the standard curve. The linear range of  $\text{H}_2\text{O}_2$  was 1.9–1670  $\mu\text{M}$ , and the LOD was 0.633  $\mu\text{M}$ , showing high selectivity and stability.

## 5.2 Biomedical therapies

The basic mechanism of POMOF materials therapy is that it has POD-like activity. When the body is exposed to various harmful stimuli, sometimes endogenous ROS may be insufficient, and the oxidative and antioxidant systems may be imbalanced, leading to tissue damage.<sup>102</sup> POMOF materials not only provide  $\text{H}_2\text{O}_2$  but also provide enough ROS with POD-like activity to destroy DNA molecules of foreign substances and thus produce a defence effect, thus effectively regulating the balance of ROS in the body.<sup>103</sup> POMOF materials can be used

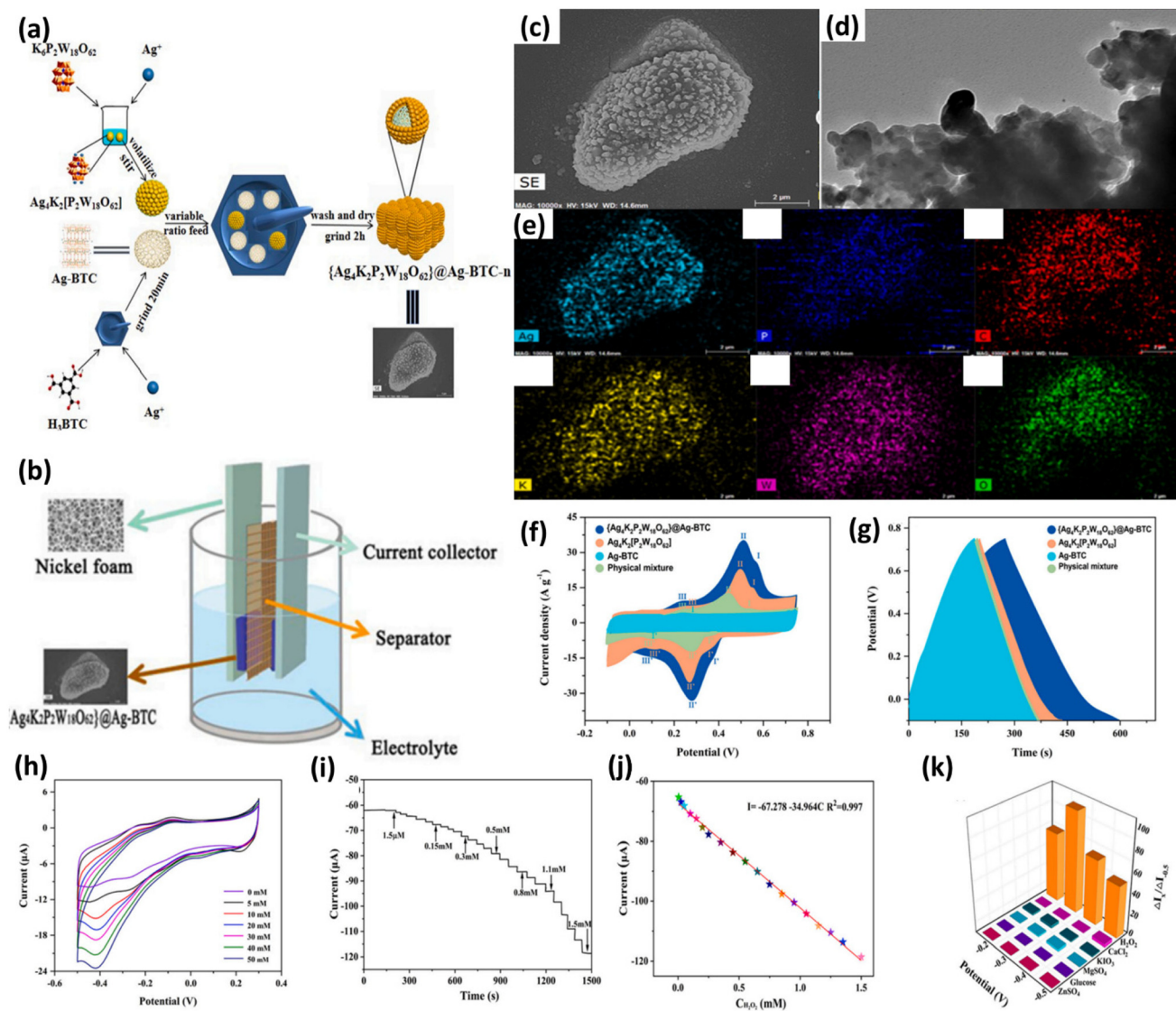


**Fig. 8** Applications of the  $\text{Ag}_4\text{K}_2\text{P}_2\text{W}_{18}\text{O}_{62}@Ag\text{-BTC-}n$  in the detection of  $\text{H}_2\text{O}_2$ . (a) Schematic illustration of the synthesis of  $\text{Ag}_4\text{K}_2\text{P}_2\text{W}_{18}\text{O}_{62}@Ag\text{-BTC-}n$ . (b) Schematic illustration of a symmetrical two-electrode system for detecting  $\text{H}_2\text{O}_2$ . (c) SEM of  $\text{Ag}_4\text{K}_2\text{P}_2\text{W}_{18}\text{O}_{62}@Ag\text{-BTC-}n$ . (d) TEM of  $\text{Ag}_4\text{K}_2\text{P}_2\text{W}_{18}\text{O}_{62}@Ag\text{-BTC-}n$ . (e) EDX plots of Ag, P, C, K, W and O. (f) CV curves of four materials. (g) GCD curves of four materials. (h) CV curves for different amounts of  $\text{H}_2\text{O}_2$  added to the test solution. (i) Current response obtained when  $\text{H}_2\text{O}_2$  is added. (j) Linear current data graph of  $\text{H}_2\text{O}_2$  concentration. (k) The influence of five interferents on the selectivity of detection.<sup>41</sup> Copyright 2022, Elsevier.

as adsorbent and loading materials for biomedical therapy, and their good biocompatibility allows them to be widely used in living organisms.<sup>104</sup>

**5.2.1 Anti-tumours.** Tumours represent a prevailing and life-threatening health concern, posing a significant biomedical challenge in contemporary times.<sup>105</sup> Secondary bacterial infections are a common issue associated with tumours, often necessitating the simultaneous administration of anti-inflammatory and anti-tumour therapies in clinical settings.<sup>106</sup> There are many ways to treat cancer: CDT, PDT (photodynamic therapy), PTT, RT (radiation therapy), EDT, *etc.* In recent years, the advancement of POMOF materials has introduced these novel approaches to tumour treatments.

**5.2.1.1 PTT and CDT.** PTT is the use of materials with high photothermal conversion efficiency or strong ROS yield exposed to a specific wavelength of the light source and its target recognition technology to allow the material to produce phototoxicity to specific tumour cells to achieve therapeutic effects. At the same time, phototherapy has been shown to kill a variety of microorganisms.<sup>108</sup> The development and utilisation of POMOF materials combine PTT and CDT to work together to treat tumours.

Our group synthesised W-POM NCs@HKUST-1 by impregnation method to bring a new means of tumour therapy.<sup>46</sup> First, phosphotungstic acid and gallic acid are combined to synthesise W-POM NCs, which are then incorporated into the



HKUST-1 framework. The resulting encapsulated structure allows the POM materials to exhibit excellent PTT therapeutic performance, while the MOF framework enhances the overall system's POD-like activity and strengthens its physical structure. In subsequent simulations under simulated physiological conditions, it was found that there was no significant aggregation in fetal bovine serum culture medium even after seven days, indicating the exceptional stability of the newly synthesized W-POM NCs@HKUST-1 and suggesting its excellent biocompatibility. W-POM NCs@HKUST-1, due to its excellent POD-like activity, exhibits superior targeted therapeutic properties. When combined with PTT and CDT, it shows high stability and an impressive photothermal conversion efficiency of up to 39.38% under near-infrared light irradiation. Fig. 9 shows the mechanism of POMOFs. It also effectively catalyzes the production of hydroxyl radicals within cells, an outstanding effect attributed to the excellent performance of W-POM NCs. The composite material demonstrates greater efficacy in killing cells compared to single therapy strategies, and the HKUST-1 framework additionally reduces the photodegradation of the photothermal materials. The composite material exhibits higher lethality than single therapeutic strategies. The utilisation of POMOF materials significantly amplifies cancer cell treatment efficacy and targeting precision. This study extends the POMOF composite nanomaterials and provides a reliable and promising means to improve tumour therapy.

Wang *et al.* engineered ZCPH nanoparticles (NPs), a versatile nanoplatform integrating PTT, anti-inflammatory, and anti-autophagy attributes for ovarian cancer intervention.<sup>49</sup> The synthesis strategy is to encapsulate POMs and chloroquine phosphate (CQ) into the ZIF-8 framework by solvothermal method, and then wrap it in hyaluronic acid (HA) to form an inclusion structure, targeting effective ovarian cancer therapy and inflammation mitigation. The study underscores the potential of non-invasive PTT as a tumour-targeting modality,

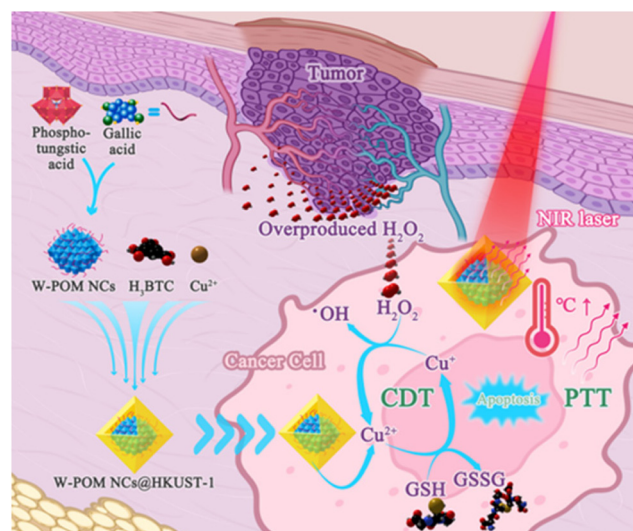


Fig. 9 Schematic illustration of the PTT and CDT mechanism of W-POM NCs@HKUST-1.<sup>46</sup> Copyright 2022, John Wiley and Sons.

inflicting nominal collateral damage to tissue *via* controllable irradiation. The nanocomposite exhibits a photothermal conversion therapeutic efficacy of up to 30.8% under an 808 nm near-infrared laser and has excellent anti-inflammatory effects based on POD-like activity in scavenging ROS in the tumour environment. In terms of biocompatibility, for SKOV3 cells treated at different concentrations, due to the synergistic effect of CQ, more than 80% of normal cells can survive even at concentrations as high as  $100 \mu\text{g mL}^{-1}$ , while tumour cells will absorb more CQ enabling ZCPHs to exert targeted cytotoxicity on tumour cells with high uptake of CQ. While performing targeted elimination of tumour cells, it also enhances the biocompatibility of the material. This study also used pH-responsive CQ to inhibit autophagy in lysosomes, cut off the self-defence mechanism “autophagy” induced by cell necrosis, and achieve collaborative treatment of tumours.

**5.2.1.2 EDT and CDT.** CDT, a new class of oncology treatment techniques based on endogenous chemical product transformation reactions in tumours, is often used in conjunction with PTT for tumours as an effective treatment.<sup>107</sup> Its mechanism of action involves catalysing the transformation of weakly oxidizing  $\text{H}_2\text{O}_2$  into potent oxidizing ROS, which escalates intracellular oxidation, provokes DNA necrosis, deactivates proteins, oxidizes lipids, and culminates in the apoptotic demise of cancer cells. CDT has been a prominent research subject in cancer therapy in recent years because of its specificity and independence and its applicability to treating tumours deep in tissues.<sup>109</sup> The disadvantages of conventional ROS therapy and its application are also affected by TME (tumour microenvironment) due to the lack of endogenous  $\text{H}_2\text{O}_2$  and GSH (glutathione) overexpression.<sup>110</sup> POMOF materials not only provide endogenous  $\text{H}_2\text{O}_2$  but also have strong POD-like activity, thus enabling the development of novel enhanced chemokinetic therapies based on POMOF materials.

Our group synthesised POM@ZIF-8 NPs by hydrothermal method. POM@ZIF-8 NPs combine EDT and CDT for tumour treatment.<sup>47</sup> The structure involves POMs being incorporated into the ZIF-8 framework to exert their effect, where the mechanism involves  $\text{W}^{5+}$  decomposing  $\text{H}_2\text{O}_2$  into  $\cdot\text{OH}$  *via* the Fenton-like reaction, collectively targeting tumour cells. The mechanism (Fig. 10) is the presence of strong POD-like activity of POM@ZIF-8 NPs and the fact that it protects normal tissues and avoids side effects due to the reaction of ZIF-8 to acid. As a result, a high degree of tumour suppression was observed *in vitro* and *in vivo*. With the influence of HeLa cells in a simulated biological microenvironment, POM@ZIF-8, even at concentrations as high as  $100 \mu\text{g mL}^{-1}$ , showed no significant damage to the cells. After 24 hours, the drug release effect remained pronounced, reflecting the exceptional biocompatibility of POMOF materials. This study provides an alternative method for a combination treatment modality with specific efficacy.

Our group also synthesised POM- $\text{CaO}_2$ @ZIF-8 by one-pot method for electro-enhanced CDT.<sup>48</sup> The synthesised POMs and  $\text{CaO}_2$  NPs are co-encapsulated within MOF frameworks,

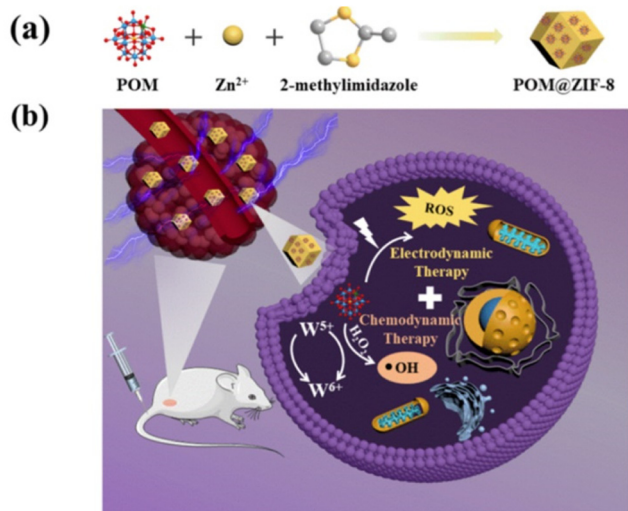


**Fig. 10** Applications of the POM@ZIF-8 NPs in EDT and CDT. (a) Schematic illustration of the synthesis of POM@ZIF-8 NPs. (b) Schematic illustration of the anticancer mechanism of POM@ZIF-8 NPs.<sup>47</sup> Copyright 2022, American Chemical Society.

forming an integrated encapsulated structure. The interaction of  $\text{CaO}_2$  with water generates  $\text{H}_2\text{O}_2$ , addressing the issue of endogenous oxygen deficiency.  $\text{W}^{5+}$  ions' main function is to convert  $\text{H}_2\text{O}_2$  into  $\text{W}^{6+}$  and  $\cdot\text{OH}$  based on electrical response, with the hydroxyl radicals acting upon tumour cells. Concurrently,  $\text{W}^{6+}$  can also decompose GSH into GSSH, thereby creating a synergistic therapeutic effect. POMOFs, when interacting with HeLa cells for more than 48 hours, continue to demonstrate effective drug release. Moreover, when interacting with mouse tumour cells, due to the supportive structure of the MOF framework, they exhibit superior stability compared to the action of POMs, and a noticeable reduction in tumour cell size is observed. The mechanism (Fig. 11) of

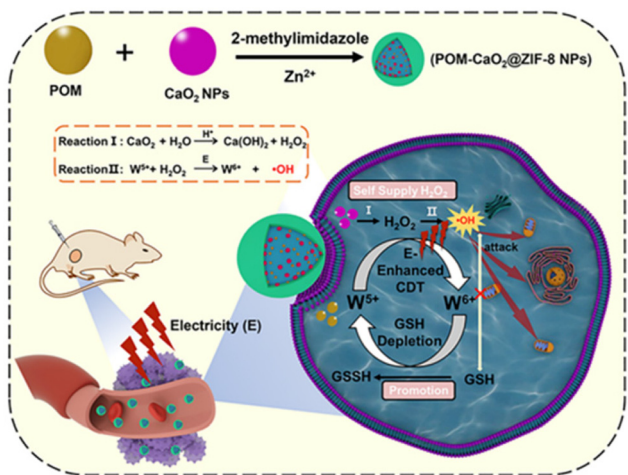


**Fig. 11** Schematic illustration of the synthesis of POM- $\text{CaO}_2$ @ZIF-8 NPs and the endogenous and exogenous enhanced CDT therapy of the tumour.<sup>48</sup> Copyright 2022, John Wiley and Sons.

POMOFs is the presence of strong POD-like activity of POM- $\text{CaO}_2$ @ZIF-8, while the simultaneous modulation of endogenous ( $\text{H}_2\text{O}_2$  produced by  $\text{CaO}_2$  NPs and GSH consumed by POM) and exogenous Fenton-like responses enhanced by electrical stimulation will have better therapeutic results. This therapeutic strategy has shown excellent tumour cell-killing effects *in vitro* and *in vivo* studies.

**5.2.2 Anti-bacterial.** Bacterial infections are a significant cause of human disease.<sup>111</sup> Using natural products or chemically modified natural antibiotics that disrupt bacterial cell membranes, prevent protein synthesis and expression, and hinder DNA replication is the traditional approach to treating bacterial infections and diseases.<sup>112</sup> Unfortunately, due to the misuse of antibiotics, viruses have significantly increased their ability to resist antibiotics, and even super viruses have emerged.<sup>113</sup> *Escherichia coli* is the most common Gram-negative bacterium.<sup>114</sup> *M. albican* (*Monilia albican*) is the most common human pathogen, causing mucosal and systemic infections with high mortality.<sup>115</sup> Axial Xanthomonas campestris is the pathogen of citrus ulcers, which can cause leaf and premature fruit drop and cause significant production losses worldwide.<sup>116</sup> POMOF materials offer a novel approach for treating these three bacterial strains.

Zheng *et al.* synthesised novel POMOF materials by one-pot self-assembly method  $[\text{Ag}_3(\text{H}_2\text{O})(\text{L})_2](\text{H}_2\text{PMO}_{12}\text{O}_{40})\cdot\text{H}_2\text{O}$  (HL = 4-(1H-1,2,4-triazole-1-methyl) benzoic acid) for antibacterial treatment.<sup>50</sup> The structure of POMOFs is formed by the interaction of Ag ions with organic ligands, creating a U-shaped linkage that constitutes a unique structural model (Fig. 12). The mechanism is that the POMOFs better stimulate the active

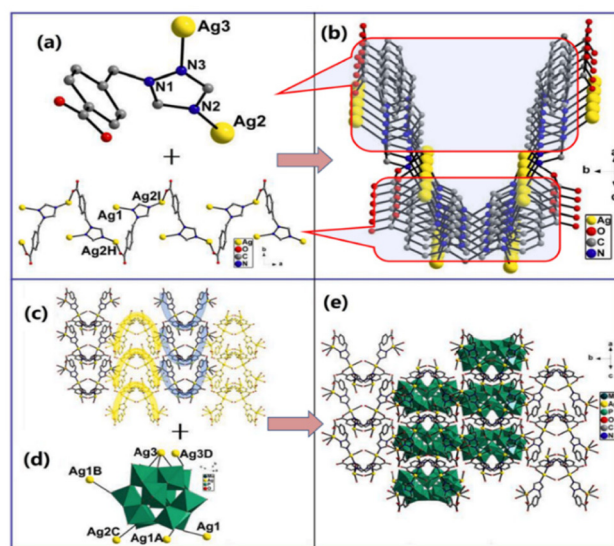


**Fig. 12** Applications of the  $\text{PMO}_{12}$ @MOF in anti-bacterial. (a) The coordination modes of organic ligands. (b) The U-shaped structural channels of POMOFs materials. (c) The U-shaped channels are arranged to form rows in turn. (d) the coordination modes of  $\{\text{PMO}_{12}\}$ . (e)  $\mu_6$ - $\{\text{PMO}_{12}\}$  ions connect the adjacent U-shaped channels to form a 3D framework.<sup>50</sup> Copyright 2022, Elsevier.



component of Ag to play POD-like activity to trigger the oxidative stress of the cell and cause the increase of intracellular ROS level. The increased ROS will damage the DNA molecules of bacteria and thus play an antibacterial role. POMOF, as a functionalised material, can effectively stimulate the action of the active component, and therefore, POMOF material is a potential antibacterial material. In the realm of antibacterial applications, POMOF materials exhibit substantial potential as medical components. Moving forward, these materials could find utility as portable medical adjuncts, a perspective that will be further explored in the subsequent prospects.

**5.2.3 Enhanced enzyme therapy.** Enzymes are excellent therapeutic agents. They can react precisely and rapidly in tiny amounts at physiological pH and body temperature.<sup>117</sup> To date, enzyme therapy has been widely used in biomedical therapeutic areas, with high-purity enzymes playing an important role in cancer treatment, inflammation therapy, gastrointestinal diseases, and kidney dysfunction.<sup>118</sup> However, due to the relatively limited conditions under which enzyme therapy operates, it is challenging to use it more effectively in combination with therapies such as PTT and CDT for treating diseases.<sup>119</sup> In recent years, the therapeutic properties of enzymes have often improved by (1) soluble chemical modification. (2) Insoluble chemical modification or immobilisation on a surface. (3) Encapsulation of enzymes into capsules of biodegradable or inert substances. POMOF materials provide a method as carriers for enzyme therapeutics, which can effectively improve thermal stability and recoverability.

An *et al.* developed a POMOF material as an adsorbent for enzyme (MP-11) encapsulation, providing an effective strategy to enhance enzyme therapy.<sup>51</sup> Fig. 13 shows the comparison of storage, release and enzyme activity of POMOF materials under different conditions. In the end, the MP-11&PW<sub>12</sub>@UiO-67 system performed best. In this study, Keggin-type phosphotungstic acid (PW<sub>12</sub>) encapsulated in a zirconium metal-organic framework (PW<sub>12</sub>@UiO-67) was used as a non-homogeneous adsorbent for enzyme encapsulation in that study. POMs are orderly filled into MOF metal frameworks and exert a charge attraction similar to magnets on the enzymes filled in other frameworks. This greatly enhances the adsorption of enzymes and facilitates the release of MP-11 at specific sites. The experimental results demonstrated that POMOF complex clusters could enhance enzyme adsorption, and the stability of MP-11 was significantly improved after immobilisation.

**5.2.4 Enhanced macrophage action.** Macrophages are widely present in vertebrates involved in non-specific defence (innate immunity) and specific defence (cellular immunity).<sup>120</sup> Their main functions are phagocytosis (*i.e.*, phagocytosis as well as digestion) of cellular debris and pathogens in the form of fixed or free cells and activation of lymphocytes or other immune cells to respond to pathogens. Some drug delivery can be targeted through macrophages.<sup>121</sup> POMOF materials provide a promising method of acting on macrophages that can be applied for drug delivery.

Roch-Marchal *et al.* prepared the material POM@MIL-101 by one-pot self-assembly method.<sup>52</sup> The structure of POMOFs

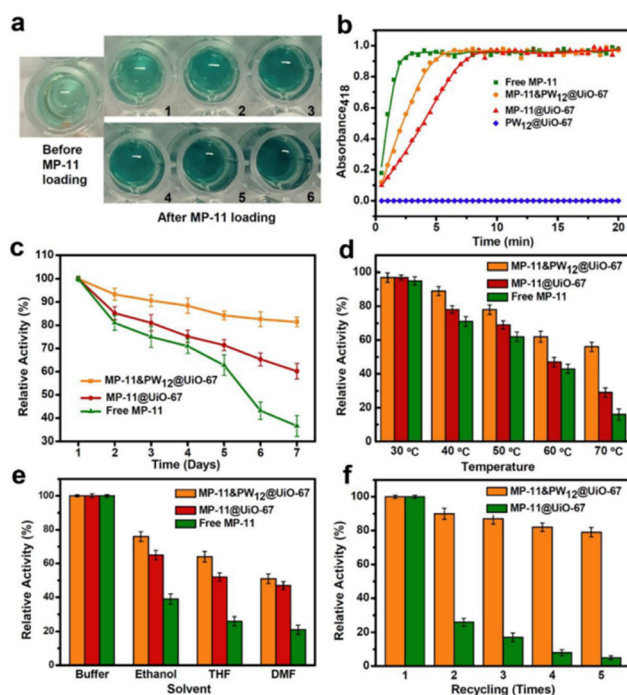


**Fig. 13** Applications of the PW<sub>12</sub>@UiO-67 in enzyme therapy. (a) Colour variations of PW<sub>12</sub>@UiO-67. (b) Catalysis trace diagram. (c) Storage stability of the system. (d) Thermal stability of the system. (e) Organic solvent stability diagram. (f) Recyclable stability diagram.<sup>51</sup> Copyright 2022, American Chemical Society.

is created by embedding POM materials into MOF frameworks, forming an integrated filled structure. Moreover, in comparison with the control group, even after a prolonged period of interaction, the internalization effect was well-distributed with no significant aggregation observed. This study found that the POM@MIL-101 complex exhibited excellent biostability and was rapidly internalised in macrophages, as observed in fluorescence confocal microscopy. The capability to be observed *via* fluorescence confocal microscopy enhances the potential of these POMOF materials as therapeutic diagnostic agents, ideal for exploring drug delivery pathways and applications. Although this study does not provide specific case studies, it offers a promising strategy for drug delivery targeting macrophages.

**5.2.5 Degradation of antibiotics.** Antibiotics are antimicrobial agents with antibacterial or bactericidal effects. The mechanism is to inhibit bacterial cell wall synthesis, enhance bacterial cell membrane permeability, interfere with bacterial protein formation, and inhibit bacterial nucleic acid replication and transcription to achieve the effect of antibacterial and bactericidal.<sup>122</sup> However, the misuse of antibiotics has been particularly serious in recent years, especially in farm animal feeds, resulting in reduced disease resistance in farm animals, increased drug resistance in pathogenic bacteria, drug residues in products, and food safety hazards, so effective degradation of antibiotics has an essential position in the biomedical field. POMOF materials provide a new strategy for degrading antibiotics.



Yang *et al.* synthesised PMA@ZIF-67 for the degradation of levofloxacin by impregnation method.<sup>53</sup> The structure of POMOF materials has led to the formation of a layered, hollow bimetallic oxide nanocage. The mechanism lies in the fact that PMA@ZIF-67 exerts POD-like activity to promote the production of ROS substances, which can effectively promote the degradation of levofloxacin and improve the catalytic activity. This study provides the design of POM@MOF hetero-derived hierarchical hollow nanocages with high peroxymonosulfate activation capacity for antibiotic removal.<sup>123</sup> Even after six cycles of reuse, POMOFs still exhibit a degradation rate of 84.7%, thereby demonstrating exceptional stability in terms of efficacy. It gave a new strategy of POMOF materials for the degradation of antibiotics.

Lan *et al.* synthesised the POM@MIL-101 material to effectively adsorb and degrade the cationic antibiotic tetracycline by solvothermal method.<sup>54</sup> The synthesised POMOFs are structured with POMs encapsulated within MOFs, forming an integrated whole. The mechanism involves POM@MIL-101 exhibiting POD-like activity to promote the degradation of tetracycline, thereby enhancing its catalytic activity. This study found that the POMOFs exhibited high degradability with a

high adsorption capacity of 912.5 mg g<sup>-1</sup>. The antibiotics adsorbed can be photodegraded, thus allowing POM@MIL-101 to be reused. POMOFs offer a novel approach to the adsorption and photodegradation of antibiotics.

**5.2.6 Separation of cytochrome C.** Cytochrome C (Cyt-C) is commonly used clinically as an adjunct to emergency treatment of hypoxia in various tissues, such as carbon monoxide poisoning, hypnotic poisoning, cyanide poisoning, neonatal asphyxia, hypoxia during severe shock, cerebrovascular accidents, post-concussion, respiratory distress due to anaesthesia and pulmonary diseases, and myocardial hypoxia due to various cardiac disorders.<sup>124</sup> Cyt-C is generally prepared by centrifugal separation of Cyt-C from the porcine heart. POMOF materials developed a new method to isolate and purify Cyt-C because of its stronger adsorption properties.

TeW<sub>6</sub>@ZIF-8 was synthesised by the impregnation method (Fig. 14) by Zhang *et al.*<sup>55</sup> The synthesis relies on the self-assembly of POMs and MOF materials, with the POMs being dispersed around the MOF framework to form a composite. TeW<sub>6</sub>@ZIF-8 composite had good biocompatibility, the Cyt-C adsorption behaviour was consistent with the Langmuir adsorption model, the theoretical adsorption capacity was

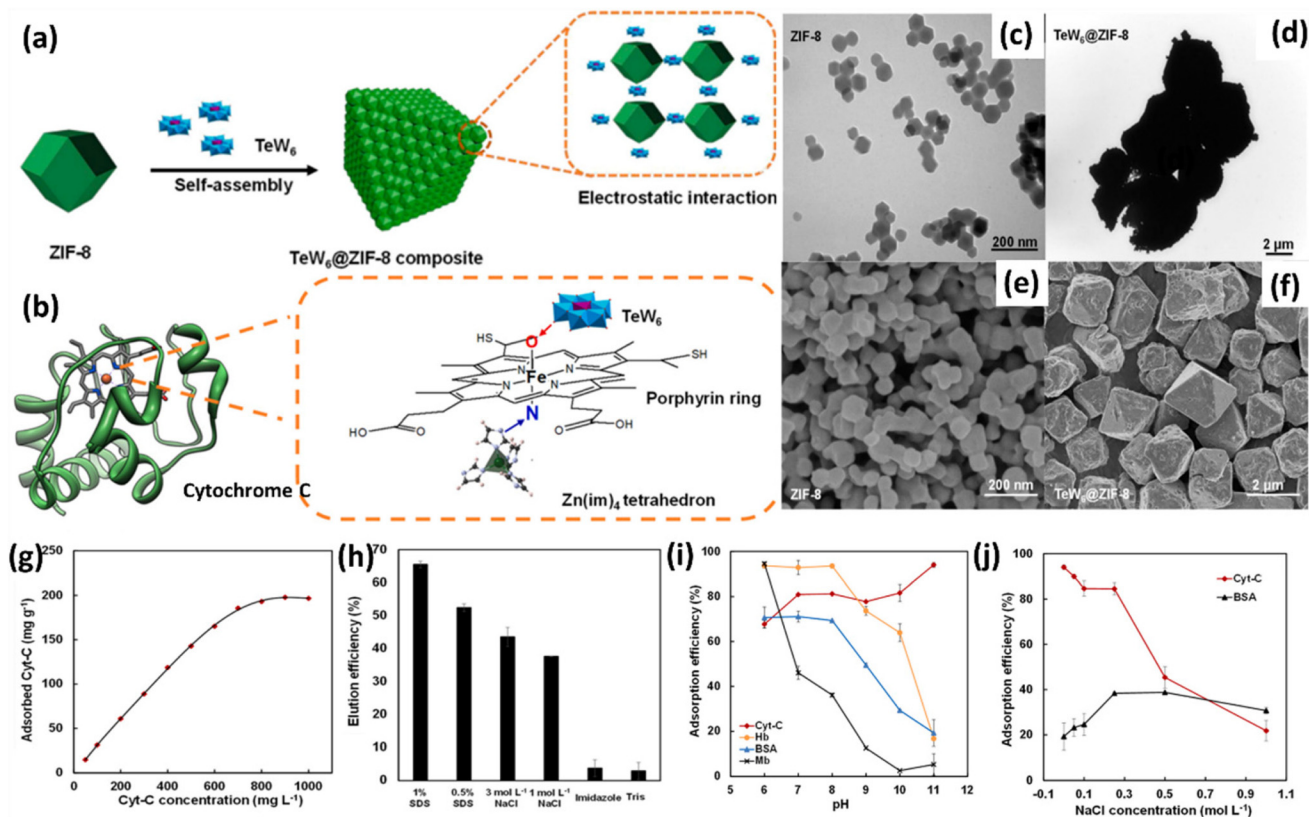


**Fig. 14** Applications of the TeW<sub>6</sub>@ZIF-8 in separation of Cyt-C. (a) Schematic illustration of the synthesis of TeW<sub>6</sub>@ZIF-8. (b) Interaction mechanism between cytochrome C and TeW<sub>6</sub>@ZIF-8. (c) TEM images of ZIF-8. (d) TEM images of TeW<sub>6</sub>@ZIF-8. (e) SEM images of ZIF-8. (f) SEM images of TeW<sub>6</sub>@ZIF-8. (g) The adsorption isotherm of Cyt-C on the TeW<sub>6</sub>@ZIF-8. (h) The recoveries of the adsorbed Cyt-C from TeW<sub>6</sub>@ZIF-8 using various buffers. (i) pH-dependent adsorption behaviours on TeW<sub>6</sub>@ZIF-8 surface. (j) Effect of ionic strength on TeW<sub>6</sub>@ZIF-8 adsorption efficiency.<sup>55</sup> Copyright 2022, Elsevier.

232.56 mg g<sup>-1</sup>, and the retained Cyt-C was easily recovered. The method achieved a recovery of 65.6% and a high adsorption efficiency of 94.01%. Therefore, the TeW<sub>6</sub>@ZIF-8 complex can be used as a novel adsorbent for the isolation and purification of Cyt-C from porcine hearts. This study gives a new research direction for POMOF materials as adsorbent materials.

## 6 Challenges and prospects

### 6.1 Challenges

For the extensive integration of POMOF materials into the biomedical realm, a meticulous examination of the pivotal constraints obstructing their transition from laboratory investigations to clinical trials is imperative. These constraints centre on the aspects of production and utilisation conditions.<sup>125</sup> Only through meticulous control over the synthesis and modification of POMOF materials can their industrial-scale production be advanced, paving the way for their formal implementation within the realm of biomedicine.<sup>126</sup> The constraints imposed by utilisation conditions are equally crucial. If POMOF materials fail to manifest catalytic activity within regular physiological parameters and lack inherent biodegradability, their viability in the realm of biomedicine will be considerably curtailed. The subsequent discussion delineates the challenges confronted by POMOF materials about the aforementioned aspects, followed by suggested avenues for enhancement.

**6.1.1 Challenges in the synthesis and modification strategies.** The primary synthesis and modification techniques of POMOF materials, as presented earlier, predominantly encompass liquid-phase reactions. In upcoming endeavours, a significant portion of these reactions aimed at accelerating synthesis rates will be conducted under conditions involving elevated pressure and temperature. The synthesis of POMOF materials grapples with the limited solubility of ligands within organic solvents (such as acetonitrile, methanol, pyridine, *etc.*).<sup>127</sup> Additionally, the formation of crystal phases in inorganic-organic hybrid polyacetal-based materials at higher temperatures poses challenges.<sup>128</sup> Concurrently, the reduction in viscosity and increase in ion product within the heated solvent enhances reactant diffusion and solubility. However, this phenomenon culminates in the development of interpenetrating structures, which adversely impact the formation of porous materials. Consequently, methods of synthesis and modification impose obstacles upon the efficient production of POMOF materials.<sup>129</sup>

The ionic thermal method involves the utilisation of ionic liquids as a reaction medium in non-organic solvents for the synthesis of crystalline solids.<sup>130</sup> Comprising solely of ions, ionic liquids possess a significantly high enthalpy of evaporation, rendering them suitable for POM synthesis.<sup>131</sup> The initial ionic thermal synthesis approach offers an environmentally friendly and effective avenue for crafting porous MOF materials based on POMs. Ionic liquids exhibit exceptional

attributes, including remarkable thermal stability and a broad liquid temperature range, making the ionic thermal method an optimal strategy for enhanced porous material synthesis. The ionic thermal synthesis techniques present an exciting and promising trajectory, poised to yield improved self-assembly synthesis and modification of POMOFs.

The microwave method, as a common method for synthesising nanomaterials, is also promising to be utilised to synthesise POMOF materials.<sup>132</sup> Its high-frequency electromagnetic wave oscillation can eliminate the utilisation of organic solvents and obtain POMOF materials in a greener way.<sup>133</sup> Simultaneously, the utilisation of the microwave method facilitates rapid nucleation, enhances the reversibility of coordination bonds, and optimises crystalline structure formation.

The aforementioned two approaches primarily explore the synthesis methodologies of POMOF materials, which can also be adapted for specific modifications. However, currently, the predominant focus of POMOF material modification is on surface structure alterations or the introduction of new compounds. Moving forward, the enhancement of POMOF material modification can be pursued by delving into the selection of diverse organic ligands.<sup>134</sup>

**6.1.2 Challenges in using conditions.** The potential application of POMOF materials in the biomedical field is promising. However, there are certain limitations regarding their usage conditions. The stability of POMOF materials within biological environments must be considered as a critical factor.<sup>135</sup> Given the intricate chemical reactions and physiological settings in living organisms, material stability is pivotal to preventing adverse reactions during prolonged usage. Furthermore, comprehending the degradation and metabolic pathways of POMOF materials within the body is essential to ensure their safe, controlled decomposition and elimination.<sup>136</sup> Evaluating material toxicity and potential side effects is imperative prior to clinical application, ensuring no risks to human health. Therefore, as POMOF materials advance into biomedical applications, considering these usage condition constraints is crucial for their secure and effective integration into clinical practice.<sup>137</sup> Additionally, further research is needed to understand the POD-like activity and electrochemical behaviour of POMOF materials under varying physical and chemical circumstances.<sup>138</sup> Investigating the adsorption performance of POMOF materials is also essential.<sup>139</sup> Exploring the selectivity of POMOF materials towards reaction substrates and conditions could lead to enhanced performance through adjustments such as temperature, pH, and reaction time. In summary, further research is required to comprehensively address the utilisation parameters of POMOF materials.<sup>140</sup>

### 6.2 Prospects

POMOF materials exhibit substantial potential for biomedical applications owing to their exceptional POD-like activity, high-efficiency electrocatalytic capabilities, and effective adsorption performance. Based on the perspective of the future application direction of POMOF materials, the “prospects” part is

divided into biomedical testing and biomedical therapies according to the above.

**6.2.1 Prospects in biomedical detection.** Primarily, POMOF materials exhibit promising prospects in the domains of biomedical detection.<sup>141</sup> Their structural and functional tunability enables the design of multifunctional agents for bioimaging, thereby paving novel paths for precision medicine. Notably, prevalent detection techniques employing POMOF materials predominantly leverage their POD-like activity. Hence, the possibility of substituting POMOF materials for POD enzyme-based detection emerges as a crucial consideration. Currently, the detection involving POMOF materials predominantly revolves around H<sub>2</sub>O<sub>2</sub> detection, independent of enzymatic involvement. Introducing specific oxidases, however, opens doors for decomposing substances such as cholesterol, urea, and Glc into H<sub>2</sub>O<sub>2</sub>.<sup>142</sup> Consequently, collaborative interactions with other enzyme-mimicking substances are anticipated to advance the detection of biologically active compounds significantly.<sup>143</sup>

The special properties of POMOF materials make them suitable for *in vitro* diagnostics, such as biosensors. Temperature, pH, and Cyt-C are specifically analysed above. In the future, the detection of more disease markers may also be combined with POMOF materials to detect abnormal internal environments and make sensors with specific functions. In this regard, there are development prospects for nano-robots and wearable sensors.<sup>144</sup> In the future, these materials may play an important role in early disease diagnosis and biomarker detection.

**6.2.2 Prospects in biomedical therapy.** POMOF materials exhibit remarkable potential as biotherapeutic agents, particularly in various therapeutic modalities, including CDT, PDT, PTT, RT, and EDT.<sup>145</sup> Furthermore, their robust adsorption and catalytic capabilities underscore their significant contributions to forthcoming drug delivery and controlled release strategies. Moreover, these materials can be seamlessly integrated into targeted therapies to enable precise treatment, mitigating the negative impact on healthy cells during tumour intervention. The subsequent analysis delves into specific insights gleaned from the preceding discourse.<sup>146</sup>

The first prospect pertains to targeted drug delivery. Currently, the utilisation of POMOF materials for targeted drug delivery remains an underexplored area.<sup>147</sup> The remarkable porous structure and high surface area of POMOF materials offer substantial potential for efficient drug encapsulation and controlled release, rendering them pivotal in the realm of drug delivery.<sup>148</sup> These materials can serve as adept drug carriers to facilitate directed delivery and regulated drug release, thereby enhancing therapeutic efficacy while mitigating toxic and adverse effects. In the context of site-specific targeted drug delivery, the manipulation of surface properties and functionalities of POMOF materials holds promise for achieving precise and focused therapeutic interventions.<sup>149</sup> This advancement is poised to enhance treatment precision, optimise therapeutic outcomes, and minimise collateral harm to healthy cells, ultimately leading to an improved therapeutic experience for patients.

The specific approach to achieve this involves initiating targeted drug delivery using POMOF materials under external stimuli such as magnetic fields and acoustic waves. By modulating the drug release rate based on specific conditions, precise control over drug administration can be attained. This approach can also be integrated with smart wearable devices to enhance the convenience of targeted drug delivery.<sup>150</sup> Furthermore, nanoparticle technology can be leveraged to fabricate nano-sized POMOF drug carriers, such as nanoparticles and nanosheets. These carriers can efficiently transport drugs to specific lesions through passive or active targeting mechanisms, enhancing drug accumulation at the intended site.<sup>151</sup>

In the context of biomedical treatment, POMOF materials exhibit promising potential. Firstly, remarkable redox performance, biocompatibility, and mechanical strength position POMOFs as potential wound suture materials to facilitate healing processes. Furthermore, POMOF materials can find application in various tumour treatments such as PDT, PTT, and RT.<sup>152</sup> Through the modulation of their optical and thermal properties, POMOF materials can effectively concentrate light or heat energy onto tumour regions, achieving targeted and selective tumour destruction.<sup>153</sup> Moreover, POMOF materials hold great promise as radiation therapy sensitisers, augmenting tumour cell sensitivity to radiation and enhancing the efficacy of radiation therapy. The realisation of this objective can be synergistically coupled with PTT and PDT through the utilisation of nanorobots.<sup>144</sup> This integration is anticipated to inaugurate a novel domain of nanorobot manipulation, propelling the emergence of cutting-edge medical apparatuses characterised by organelle-level resolution.<sup>154</sup> Such advancements herald a new era of medical machinery, facilitating the attainment of personalised medicine tailored to the distinctive requirements of individual patients.<sup>155</sup> This encompasses tailored drug delivery systems and therapeutic regimens, thereby offering a comprehensive and adaptable approach. POMOF materials may also extend to wearable technology and health monitoring, furnishing a more exact and sensitive platform for health surveillance.

## Author contributions

Lijin Wang: investigation, visualization; Pengyu Dai: data curation, writing-original draft; Hongli Ma: conceptualization, software; Tiedong Sun: writing-reviewing and editing; Jinsong Peng: supervision.

## Conflicts of interest

There are no conflicts to declare.

## Acknowledgements

This work was funded by the National Natural Science Foundation of China (No. 52372264) and the Natural Science Foundation of Heilongjiang Province (No. LH2023B002).



## References

- C. Pettinari, R. Pettinari, C. Di Nicola, A. Tombesi, S. Scuri and F. Marchetti, Antimicrobial MOFs, *Coord. Chem. Rev.*, 2021, **446**, 214121.
- Z. J. Chen, K. O. Kirlikovali, P. Li and O. K. Farha, Reticular Chemistry for Highly Porous Metal-Organic Frameworks: The Chemistry and Applications, *Acc. Chem. Res.*, 2022, **55**, 579–591.
- X. Zhang, Z. J. Chen, X. Y. Liu, S. L. Hanna, X. J. Wang, R. Taheri-Ledari, A. Maleki, P. Li and O. K. Farha, A historical overview of the activation and porosity of metal-organic frameworks, *Chem. Soc. Rev.*, 2020, **49**, 7406–7427.
- W. B. Liang, P. Wied, F. Carraro, C. J. Sumbly, B. Nidetzky, C. K. Tsung, P. Falcaro and C. J. Doonan, Metal-Organic Framework-Based Enzyme Biocomposites, *Chem. Rev.*, 2021, **121**, 1077–1129.
- J. J. Chen, Y. F. Zhu and S. Kaskel, Porphyrin-Based Metal-Organic Frameworks for Biomedical Applications, *Angew. Chem., Int. Ed.*, 2021, **60**, 5010–5035.
- M. J. Hao, M. Q. Qiu, H. Yang, B. W. Hu and X. X. Wang, Recent advances on preparation and environmental applications of MOF-derived carbons in catalysis, *Sci. Total Environ.*, 2021, **760**, 143333.
- A. J. Howarth, Y. Y. Liu, P. Li, Z. Y. Li, T. C. Wang, J. Hupp and O. K. Farha, Chemical, thermal and mechanical stabilities of metal-organic frameworks, *Nat. Rev. Mater.*, 2016, **1**, 1–15.
- H. D. Lawson, S. P. Walton and C. Chan, Metal-Organic Frameworks for Drug Delivery: A Design Perspective, *ACS Appl. Mater. Interfaces*, 2021, **13**, 7004–7020.
- L. J. Xu, C. M. Wang, K. Yu, C. X. Wang and B. B. Zhou, Research progress of POMs constructed by 1,3,5-benzenetricarboxylic acid: From synthesis to application, *Coord. Chem. Rev.*, 2023, **481**, 215044.
- H. R. He, P. Xu, D. M. Wang, H. W. Zhou and C. H. Chen, Polyoxometalate-modified halloysite nanotubes-based thin-film nanocomposite membrane for efficient organic solvent nanofiltration, *Sep. Purif. Technol.*, 2022, **295**, 121348.
- Z. Y. Han, X. Y. Li, Q. Li, H. S. Li, J. Xu, N. Li, G. X. Zhao, X. Wang, H. L. Li and S. D. Li, Construction of the POMOF@Polypyrrole Composite with Enhanced Ion Diffusion and Capacitive Contribution for High-Performance Lithium-Ion Batteries, *ACS Appl. Mater. Interfaces*, 2021, **13**, 6265–6275.
- S. J. Yu, H. W. Pang, S. Y. Huang, H. Tang, S. Q. Wang, M. Q. Qiu, Z. S. Chen, H. Yang, G. Song, D. Fu, B. W. Hu and X. X. Wang, Recent advances in metal-organic framework membranes for water treatment: A review, *Sci. Total Environ.*, 2021, **800**, 149662.
- M. I. S. Verissimo, D. V. Evtuguin and M. Gomes, Polyoxometalate Functionalized Sensors: A Review, *Front. Chem.*, 2022, **10**, 840657.
- K. Maru, S. Kalla and R. Jangir, MOF/POM hybrids as catalysts for organic transformations, *Dalton Trans.*, 2022, **51**, 11952–11986.
- L. Wang, A. N. Wang, Z. Z. Xue, Y. R. Wang, S. D. Han and G. M. Wang, In situ growth of polyoxometalate-based metal-organic framework nanoflower arrays for efficient hydrogen evolution, *Chin. Chem. Lett.*, 2023, **34**, 107414.
- J. Li, R. Wang, Z. Y. Dong, X. J. Zhang, X. Li, Y. T. Li and Z. M. Su, Postdecorated Polyoxometalate Metal-Organic Framework-Constructed Ternary Electrocatalysts for Hydrogen Evolution, *Cryst. Growth Des.*, 2023, **23**, 6403–6409.
- Y. H. Chen, H. Y. An, S. Z. Chang, Y. Q. Li, T. Q. Xu, Q. S. Zhu, H. Y. Luo, Y. H. Huang and Y. T. Wei, Two pseudo-polymorphic porous POM-pillared MOFs for sulfide-sulfoxide transformation: Efficient synergistic effects of POM precursors, metal sites and microstructures, *Chin. Chem. Lett.*, 2023, **34**, 107856.
- C. Y. Liang, X. Wang, D. X. Yu, W. Guo, F. Zhang and F. Y. Qu, In-situ Immobilization of a Polyoxometalate Metal-Organic Framework (NENU-3) on Functionalized Reduced Graphene Oxide for Hydrazine Sensing, *Chin. J. Chem.*, 2021, **39**, 2889–2897.
- W. J. Cui, S. M. Zhang, Y. Y. Ma, Y. Wang, R. X. Miao and Z. G. Han, Polyoxometalate-Incorporated Metal-Organic Network as a Heterogeneous Catalyst for Selective Oxidation of Aryl Alkenes, *Inorg. Chem.*, 2022, **61**, 9421–9432.
- S. Wang, T. Zhang, X. Zhu, S. Zu, Z. Xie, X. Lu, M. Zhang, L. Song and Y. Jin, Metal-Organic Frameworks for Electrocatalytic Sensing of Hydrogen Peroxide, *Molecules*, 2022, **27**, 4571.
- X. L. Wang, J. J. Sun, H. Y. Lin, Z. H. Chang, G. C. Liu and X. Wang, A series of novel Anderson-type polyoxometalate-based Mn-II complexes constructed from pyridyl-derivatives: assembly, structures, electrochemical and photocatalytic properties, *CrystEngComm*, 2017, **19**, 3167–3177.
- A. M. Kaczmarek, Eu<sup>3+</sup>/Tb<sup>3+</sup> and Dy<sup>3+</sup> POM@MOFs and 2D coordination polymers based on pyridine-2,6-dicarboxylic acid for ratiometric optical temperature sensing, *J. Mater. Chem. C*, 2018, **6**, 5916–5925.
- C. Viravaux, O. Oms, A. Dolbecq, E. Nassar, L. Busson, C. Mellot-Draznieks, R. Dessapt, H. Serier-Brault and P. Mialane, Temperature sensors based on europium polyoxometalate and mesoporous terbium metal-organic framework, *J. Mater. Chem. C*, 2021, **9**, 8323–8328.
- X. Li, S. X. Li, Y. L. Wang, K. F. Zhou, P. P. Li and J. Q. Sha, Synthesis, structure and effective peroxidase-like activity of a stable polyoxometalate-pillared metal-organic framework with multinuclear cycles, *Polyhedron*, 2018, **151**, 206–212.
- X. Li, X. Y. Yang, J. Q. Sha, T. Han, C. J. Du, Y. J. Sun and Y. Q. Lan, POMOF/SWNT Nanocomposites with Prominent Peroxidase-Mimicking Activity for L-Cysteine “On-Off Switch” Colorimetric Biosensing, *ACS Appl. Mater. Interfaces*, 2019, **11**, 16896–16904.
- X. Li, L. J. Sun, X. Y. Yang, K. F. Zhou, G. G. Zhang, Z. B. Tong, C. Wang and J. Q. Sha, Enhancing the colorimetric detection of H<sub>2</sub>O<sub>2</sub> and ascorbic acid on polypyrrole

- coated fluconazole-functionalized POMOFs, *Analyst*, 2019, **144**, 3347–3356.
- 27 Y. Y. Wang, H. F. Zhang, D. H. Wang, N. Sheng, G. G. Zhang, L. Yin and J. Q. Sha, Development of a Uricase-Free Colorimetric Biosensor for Uric Acid Based on PPy-Coated Polyoxometalate-Encapsulated Fourfold Helical Metal-Organic Frameworks, *ACS Biomater. Sci. Eng.*, 2020, **6**, 1438–1448.
- 28 Q. Li, M. Xu, X. Li, S. Li, L. Hou, Y. Chen and J. Sha, A polypyrrole-coated eightfold-helical Wells-Dawson POM-based Cu-FKZ framework for enhanced colorimetric sensing, *Analyst*, 2020, **145**, 4021–4030.
- 29 Z. B. Tong, M. Q. Xu, Q. Li, C. Liu, Y. L. Wang and J. Q. Sha, Polyelectrolyte-functionalized reduced graphene oxide wrapped helical POMOF nanocomposites for bioenzyme-free colorimetric biosensing, *Talanta*, 2020, **220**, 121373.
- 30 M. Xu, X. Li, J. Q. Sha, Z. Tong, Q. Li and C. Liu, Hollow POM@MOF-derived Porous NiMo<sub>6</sub>@Co<sub>3</sub>O<sub>4</sub> for Biothiol Colorimetric Detection, *Chem. – Eur. J.*, 2021, **27**, 9141–9151.
- 31 Y. Ji, Y. Wei, J. Shen, J. Zhuo, M. Xu, Y. Wang and J. Sha, Increasing the peroxidase-like activity of the MIL-100(Fe) nanozyme by encapsulating Keggin-type 12-phosphomolybdate and covering three-dimensional graphene, *Analyst*, 2023, **148**, 2725–2731.
- 32 X. Liu, Q. Zheng, D. Jia, W. Wang, H. Zhao, X. Tao and J. Sha, Ternary MIL-101(Fe)@P2W18@SWNT Nanocomposites as Colorimetric Biosensors with Highly Peroxidase-Like Activity, *J. Cluster Sci.*, 2023, **34**, 3095–3103.
- 33 K. Zhou, H. Han, J. Sha, S. Luan, Y. Diao, C. Dong and J. Yang, Synthesis of POMOFs with 8-fold helix and its composite with carboxyl functionalized SWCNTs for the voltammetric determination of dopamine, *Anal. Bioanal. Chem.*, 2021, **413**, 5309–5320.
- 34 W. H. Ho, T. Y. Chen, K. Otake, Y. C. Chen, Y. S. Wang, J. H. Li, H. Y. Chen and C. W. Kung, Polyoxometalate adsorbed in a metal-organic framework for electrocatalytic dopamine oxidation, *Chem. Commun.*, 2020, **56**, 11763–11766.
- 35 L. Zhang, C. Li, F. B. Li, S. B. Li, H. Y. Ma and F. Gu, A sensing platform based on Cu-MOF encapsulated Dawson-type polyoxometalate crystal material for electrochemical detection of xanthine, *Microchim. Acta*, 2023, **190**, 24.
- 36 T. W. Murinzi, G. M. Watkins, M. Shumba and T. Nyokong, Electrocatalytic detection of l-cysteine using molybdenum POM doped-HKUST-1 metal organic frameworks, *J. Coord. Chem.*, 2021, **74**, 1730–1748.
- 37 C. Wang, M. Zhou, Y. Y. Ma, H. Q. Tan, Y. H. Wang and Y. G. Li, Hybridized Polyoxometalate-Based Metal-Organic Framework with Ketjenblack for the Nonenzymatic Detection of H<sub>2</sub>O<sub>2</sub>, *Chem. – Asian J.*, 2018, **13**, 2054–2059.
- 38 L. P. Cui, K. Yu, J. H. Lv, C. H. Guo and B. B. Zhou, A 3D POMOF based on a {AsW<sub>12</sub>} cluster and a Ag-MOF with interpenetrating channels for large-capacity aqueous asymmetric supercapacitors and highly selective biosensors for the detection of hydrogen peroxide, *J. Mater. Chem. A*, 2020, **8**, 22918–22928.
- 39 Y. Liang, N. Kang, C. M. Wang, K. Yu, J. H. Lv, C. X. Wang and B. B. Zhou, A hybrid borotungstate-coated metal-organic framework with supercapacitance, photocatalytic dye degradation and H<sub>2</sub>O<sub>2</sub> sensing properties, *Dalton Trans.*, 2022, **51**, 7613–7621.
- 40 L. J. Xu, X. Y. Zhao, K. Yu, C. M. Wang, J. H. Lv, C. X. Wang and B. B. Zhou, Simple preparation of Ag-BTC-modified Co<sub>3</sub>Mo<sub>7</sub>O<sub>24</sub> mesoporous material for capacitance and H<sub>2</sub>O<sub>2</sub>-sensing performances, *CrystEngComm*, 2022, **24**, 5614–5621.
- 41 Y. Liang, S. Di, C. M. Wang, K. Yu, C. X. Wang, J. H. Lv and B. B. Zhou, Synthesis of {P2W18}-based coated structured nano materials with supercapacitors and H<sub>2</sub>O<sub>2</sub> sensing, *J. Energy Storage*, 2022, **56**, 105991.
- 42 L. Zhang, S. Di, H. Lin, C. Wang, K. Yu, J. Lv, C. Wang and B. Zhou, Nanomaterial with Core-Shell Structure Composed of {P2W18O62} and Cobalt Homobenzotriozate for Supercapacitors and H<sub>2</sub>O<sub>2</sub>-Sensing Applications, *Nanomaterials*, 2023, **13**, 1176.
- 43 Z. J. Song, L. Y. Wang, N. Kang, K. Yu, J. H. Lv and B. B. Zhou, 3D host-guest material of {Ag(pz)} modified {BW12O40} with supercapacitor, photocatalytic dye degradation and H<sub>2</sub>O<sub>2</sub> sensing performances, *J. Solid State Chem.*, 2023, **323**, 124038.
- 44 L. Xu, S. Di, H. Lin, C. Wang, C. Wang, K. Yu, J. Lv and B. Zhou, Ni<sub>3</sub>P2W18O62-Ni<sub>3</sub>(BTC)<sub>2</sub> composite of Ni<sub>3</sub>P2W18O62 coated on the surface of the Ni<sub>3</sub>(BTC)<sub>2</sub> with supercapacitor and H<sub>2</sub>O<sub>2</sub> sensing properties was prepared by simple grinding strategy, *Electrochim. Acta*, 2023, **466**, 143028.
- 45 C. Shi, S. Di, H. Jiang, C. Wang, C. Wang, K. Yu, J. Lv and B. Zhou, Host-guest compound formed by Cu<sub>3</sub>[P2W18O62] and HKUST-1 with capacitance and H<sub>2</sub>O<sub>2</sub> sensing properties, *Dalton Trans.*, 2023, **52**, 9406–9413.
- 46 J. L. Liu, M. Y. Huang, Z. Y. Hua, J. T. Ni, Y. Dong, Z. R. Feng, T. D. Sun and C. X. Chen, Synergistic combination: Promising nanoplatfrom W-POM NCs@ HKUST-1 for photothermal and chemodynamic reinforced anti-tumor therapy, *Appl. Organomet. Chem.*, 2022, **36**, e6693.
- 47 Y. Song, Y. Sun, M. L. Tang, Z. Y. Yue, J. T. Ni, J. G. Zhao, W. X. Wang, T. D. Sun, L. X. Shi and L. Wang, Polyoxometalate Modified by Zeolite Imidazole Framework for the pH-Responsive Electrodynamic/Chemodynamic Therapy, *ACS Appl. Mater. Interfaces*, 2022, **14**, 4914–4920.
- 48 T. D. Sun, Z. Y. Yue, Y. Song, J. T. Ni, W. X. Wang, J. G. Zhao, J. L. Li, Y. Sun and B. Li, One-pot synthesis of POM-CaO<sub>2</sub>@ZIF-8 nanoparticles with self-supply of H<sub>2</sub>O<sub>2</sub> for electrically enhanced chemodynamic therapy, *Appl. Organomet. Chem.*, 2022, **36**, e6888.
- 49 D. Wang, Y. Wang, X. Zhang, Q. Lv, G. Ma, Y. Gao, S. Liu, C. Wang, C. Li, X. Sun and J. Wan, A Polyoxometalate-

- Encapsulated Metal-Organic Framework Nanoplatfom for Synergistic Photothermal-Chemotherapy and Anti-Inflammation of Ovarian Cancer, *Molecules*, 2022, **27**, 8350.
- 50 Y. G. Zheng and W. Xue, A new 3D POMOF built upon Keggin clusters and flexible n-heterocycle carboxylate ligands for catalytic and antimicrobial properties, *Inorg. Chem. Commun.*, 2022, **141**, 109520.
- 51 Q. An, Z. Xu, W. Shang, Y. Wang, X. Liu, D. Guo, M. Zeng and Z. Jia, Polyoxometalate-Based Metal-Organic Frameworks as the Solid Support to Immobilize MP-11 Enzyme for Enhancing Thermal and Recyclable Stability, *ACS Appl. Bio Mater.*, 2022, **5**, 1222–1229.
- 52 C. Roch-Marchal, T. Hidalgo, H. Banh, R. A. Fischer and P. Horcajada, A Promising Catalytic and Theranostic Agent Obtained through the In situ Synthesis of Au Nanoparticles with a Reduced Polyoxometalate Incorporated within Mesoporous MIL-101, *Eur. J. Inorg. Chem.*, 2016, **2016**, 4387–4394.
- 53 X. L. Yang, X. Y. Xie, S. Q. Li, W. X. Zhang, X. D. Zhang, H. X. Chai and Y. M. Huang, The POM@MOF hybrid derived hierarchical hollow Mo/Co bimetal oxides nanocages for efficiently activating peroxymonosulfate to degrade levofloxacin, *J. Hazard. Mater.*, 2021, **419**, 126360.
- 54 Q. Lan, S. J. Jin, B. H. Yang, Z. M. Zhang, X. Y. Li, H. Q. Xie, X. L. Jin, H. Zhang and Q. Zhao, Filling Polyoxoanions into MIL-101(Fe) for Adsorption of Organic Pollutants with Facile and Complete Visible Light Photocatalytic Decomposition, *Molecules*, 2022, **27**, 3404.
- 55 Y. Zhang, D. D. Zhang, X. Wu, R. Z. Song, X. A. Zhang, M. M. Wang, S. H. He and Q. Chen, A Novel Anderson-Evans Polyoxometalate-based Metal-organic Framework Composite for the Highly Selective Isolation and Purification of Cytochrome C from Porcine Heart, *Colloids Surf., B*, 2022, **213**, 0927–7765.
- 56 M. Ranjha, B. Shafique, A. Rehman, A. Mehmood, A. Ali, S. M. Zahra, U. Roobab, A. Singh, S. A. Ibrahim and S. A. Siddiqui, Biocompatible Nanomaterials in Food Science, Technology, and Nutrient Drug Delivery: Recent Developments and Applications, *Front. Nutr.*, 2022, **8**, 778155.
- 57 R. Tian, B. Zhang, M. Zhao, Q. Ma and Y. Qi, Polyoxometalates as promising enzyme mimics for the sensitive detection of hydrogen peroxide by fluorometric method, *Talanta*, 2018, **188**, 332–338.
- 58 J. H. Ding, Y. F. Liu, Z. T. Tian, P. J. Lin, F. Yang, K. Li, G. P. Yang and Y. G. Wei, Uranyl-silicotungstate-containing hybrid building units  $\{\alpha\text{-SiW9}\}$  and  $\{\gamma\text{-SiW10}\}$  with excellent catalytic activities in the three-component synthesis of dihydropyrimidin-2(1H)-ones, *Inorg. Chem. Front.*, 2023, **10**, 3195–3201.
- 59 Q. Liu, X. H. Zhou, H. Wu and B. Zheng, Blocking-free and self-contained immunoassay platform for one-step point-of-care testing, *Biosens. Bioelectron.*, 2020, **165**, 112394.
- 60 J. Liu, M. Huang, Z. Hua, Y. Dong, Z. Feng, T. Sun and C. Chen, Polyoxometalate-Based Metal Organic Frameworks: Recent Advances and Challenges, *ChemistrySelect*, 2022, **7**, e202200546.
- 61 A. Ianiro, H. Wu, M. M. J. van Rijt, V. M. Paula, A. D. A. Keizer, A. C. C. Esteves, R. Tuinier, H. Friedrich, N. A. J. M. Sommerdijk and J. P. Patterson, Liquid-liquid phase separation during amphiphilic self-assembly, *Nat. Chem.*, 2019, **11**, 320–328.
- 62 N. M. Fhionnlaioich, S. Schrettl, N. B. Tito, Y. Yang, M. Nair, L. A. Serrano, K. Harkness, P. J. Silva, H. Frauenrath, F. Serra, W. C. Carter, F. Stellacci and S. Guldin, Reversible Microscale Assembly of Nanoparticles Driven by the Phase Transition of a Thermotropic Liquid Crystal, *ACS Nano*, 2023, **17**, 9906–9918.
- 63 Y. Wang, C. Li, L. Ma, X. Y. Wang, K. Wang, X. H. Lu and Y. L. Cai, Interfacial Liquid-Liquid Phase Separation-Driven Polymerization-Induced Electrostatic Self-Assembly, *Macromolecules*, 2021, **54**, 5577–5585.
- 64 L. Y. Wang, H. Lin, C. X. Wang, K. Yu, C. M. Wang, J. H. Lv and B. B. Zhou, Core-shell structured tungstocuprate@silver homobenzotriazolate complex for supercapacitor and oxygen evolution reaction, *J. Energy Storage*, 2023, **66**, 107398.
- 65 S. D. Su, X. M. Li, Z. Y. Liu, W. M. Ding, Y. Cao, Y. Yang, Q. Su and M. Luo, Microchemical environmental regulation of POMs@MIL-101(Cr) promote photocatalytic nitrogen to ammonia, *J. Colloid Interface Sci.*, 2023, **646**, 547–554.
- 66 Z. F. Zhang, C. J. Gomez-Garcia, Q. Wu, J. J. Xin, H. J. Pang, H. Y. Ma, D. F. Chai, S. B. Li and C. Y. Zhao, Synthesis of a Polyoxometalate-Encapsulated Metal-Organic Framework via In Situ Ligand Transformation Showing Highly Catalytic Activity in Both Hydrogen Evolution and Dye Degradation, *Inorg. Chem.*, 2022, **61**, 11830–11836.
- 67 B. Iqbal, M. Saleem, S. N. Arshad, J. Rashid, N. Hussain and M. Zaheer, One-Pot Synthesis of Heterobimetallic Metal-Organic Frameworks (MOFs) for Multifunctional Catalysis, *Chem. – Eur. J.*, 2019, **25**, 10490–10498.
- 68 T. D. Zhang, X. D. Deng, M. Y. Wang, L. L. Chen, X. T. Wang, C. Y. Li, W. P. Shi, W. J. Lin, Q. Li, W. C. Pan, X. D. Ni, T. Z. Pan and D. C. Yin, Formation of  $\beta$ -Lactoglobulin Self-Assemblies via Liquid-Liquid Phase Separation for Applications beyond the Biological Functions, *ACS Appl. Mater. Interfaces*, 2021, **13**, 46391–46405.
- 69 J. W. Song, R. R. Xing, T. F. Jiao, Q. M. Peng, C. Q. Yuan, H. Möhwald and X. H. Yan, Crystalline Dipeptide Nanobelts Based on Solid-Solid Phase Transformation Self-Assembly and Their Polarization Imaging of Cells, *ACS Appl. Mater. Interfaces*, 2018, **10**, 2368–2376.
- 70 P. L. Liao, S. H. Zang, T. Y. Wu, H. J. Jin, W. K. Wang, J. B. Huang, B. Z. Tang and Y. Yan, Generating circularly polarized luminescence from clusterization-triggered emission using solid phase molecular self-assembly, *Nat. Commun.*, 2021, **12**, 5496.



- 71 H. X. Chen, J. Y. Wu, Q. B. Xiong, X. J. Li and X. J. Huang, Efficient capture of fluoroquinolones in urine and milk samples with multi-monolith fibers solid phase microextraction based on hybrid metal-organic framework/monolith material, *Microchem. J.*, 2023, **189**, 108575.
- 72 H. Liang, D. M. Yin, L. A. Shi, Y. H. Liu, X. Hu, N. Zhu and K. Guo, Surface modification of cellulose via photo-induced click reaction, *Carbohydr. Polym.*, 2023, **301**, 120321.
- 73 S. Dissegna, K. Epp, W. R. Heinz, G. Kieslich and R. A. Fischer, Defective Metal-Organic Frameworks, *Adv. Mater.*, 2018, **30**, 1704501.
- 74 M. R. Axet, S. Castillon, C. Claver, K. Philippot, P. Lecante and B. Chaudret, Chiral Diphosphite-modified Rhodium (0) Nanoparticles: Catalyst Reservoir for Styrene Hydroformylation, *Eur. J. Inorg. Chem.*, 2008, 3460–3466.
- 75 Y. J. Luo, Y. X. Yao, P. Wu, X. H. Zi, N. Sun and J. He, The potential role of N-7-methylguanosine (m7G) in cancer, *J. Hematol. Oncol.*, 2022, **15**, 63.
- 76 S. B. Li, H. Y. Ma, H. J. Pang, L. Zhang, Z. F. Zhang and H. D. Lin, The first 3D POMOF based on alpha-metatungstate and mixed-ligand, *Inorg. Chem. Commun.*, 2014, **44**, 15–19.
- 77 T. Kang, Y. G. Kim, D. Kim and T. Hyeon, Inorganic nanoparticles with enzyme-mimetic activities for biomedical applications, *Coord. Chem. Rev.*, 2020, **403**, 213092.
- 78 C. Y. Lin, X. J. Guo, F. Y. Mo and D. P. Sun, Different Dimensional Copper-Based Metal-Organic Frameworks with Enzyme-Mimetic Activity for Antibacterial Therapy, *Int. J. Mol. Sci.*, 2023, **24**, 3173.
- 79 H. Zhang, W. L. Zhao, H. Li, Q. Zhuang, Z. Sun, D. Cui, X. Chen, A. Guo, X. Ji, S. An, W. Chen and Y. F. Song, Latest progress in covalently modified polyoxometalates-based molecular assemblies and advanced materials, *Polyoxometalates*, 2022, **1**, 9140011.
- 80 D. Zang and H. Wang, Polyoxometalate-based nanostructures for electrocatalytic and photocatalytic CO<sub>2</sub> reduction, *Polyoxometalates*, 2022, **1**, 9140006.
- 81 H. R. Tan, X. Zhou, H. Q. You, Q. Zheng, S. Y. Zhao and W. M. Xuan, A porous Anderson-type polyoxometalate-based metal-organic framework as a multifunctional platform for selective oxidative coupling with amines, *Dalton Trans.*, 2023, **52**, 17019–17029.
- 82 D. Zang, X. J. Gao, L. Li, Y. Wei and H. Wang, Confined interface engineering of self-supported Cu@N-doped graphene for electrocatalytic CO<sub>2</sub> reduction with enhanced selectivity towards ethanol, *Nano Res.*, 2022, **15**, 8872–8879.
- 83 K. Qin, D. Zang and Y. Wei, Polyoxometalates based compounds for green synthesis of aldehydes and ketones, *Chin. Chem. Lett.*, 2023, **34**, 107999.
- 84 Z. Zhou, Q. Ke, M. Wu, L. Zhang and K. Jiang, Pore Space Partition Approach of ZIF-8 for pH Responsive Codelivery of Ursolic Acid and 5-Fluorouracil, *ACS Mater. Lett.*, 2023, **5**, 466–472.
- 85 Q. Ke, P. Jing, Y. Wan, T. Xia, L. Zhang, X. Cao and K. Jiang, Sulfonated vitamin K3 mediated bimetallic metal-organic framework for multistage augmented cancer therapy, *J. Colloid Interface Sci.*, 2024, **654**, 224–234.
- 86 Y. Cheng, K.-J. Qin and D.-J. Zang, Polyoxometalates based nanocomposites for bioapplications, *Rare Met.*, 2023, **42**, 3570–3600.
- 87 B. Ding, H. Chen, J. Tan, Q. Meng, P. Zheng, P. Ma and J. Lin, ZIF-8 Nanoparticles Evoke Pyroptosis for High-Efficiency Cancer Immunotherapy, *Angew. Chem., Int. Ed.*, 2023, **62**, e202215307.
- 88 D. Y. Du, J. S. Qin, S. L. Li, Z. M. Su and Y. Q. Lan, Recent advances in porous polyoxometalate-based metal-organic framework materials, *Chem. Soc. Rev.*, 2014, **43**, 4615–4632.
- 89 Q. Zhao, X. Y. Zheng, L. Xing, Y. L. Tang, X. M. Zhou, L. Hu, W. L. Yao and Z. Q. Yan, 2D Co<sub>3</sub>O<sub>4</sub> stabilizing Rh nano composites developed for visual sensing bioactive urea and toxic p-aminophenol in practice by synergetic-reinforcing oxidase activity, *J. Hazard. Mater.*, 2021, **409**, 125019.
- 90 S. E. Son, P. K. Gupta, W. Hur, H. B. Lee, Y. Park, J. Park, S. N. Kim and G. H. Seong, Citric Acid-Functionalized Rhodium-Platinum Nanoparticles as Peroxidase Mimics for Determination of Cholesterol, *ACS Appl. Nano Mater.*, 2021, **4**, 8282–8291.
- 91 X. Cai, Y. Luo, C. Zhu, D. Huang and Y. Song, Rhodium nanocatalyst-based lateral flow immunoassay for sensitive detection of staphylococcal enterotoxin B, *Sens. Actuators, B*, 2022, **367**, 132066.
- 92 W. Y. Xiao and Q. C. Dong, The Recent Advances in Bulk and Microfluidic-Based pH Sensing and Its Applications, *Catalysts*, 2022, **12**, 1124.
- 93 C. A. Thomas, J. S. Lee, R. J. Bernardo, R. J. Anderson, V. Glinskii, Y. K. Sung, K. Kudelko, H. Hedlin, A. Sweatt, S. M. Kawut, R. Raj, R. T. Zamanian and V. D. Perez, Prescription Patterns for Pulmonary Vasodilators in the Treatment of Pulmonary Hypertension Associated With Chronic Lung Diseases: Insights From a Clinician Survey, *Front. Med.*, 2021, **8**, 764815.
- 94 M. R. R. Khan and S. W. Kang, Highly Sensitive and Wide-Dynamic-Range Multichannel Optical-Fiber pH Sensor Based on PWM Technique, *Sensors*, 2016, **16**, 1885.
- 95 J. B. Yu, E. Lewis, G. Brambilla and P. F. Wang, Temperature Sensing Performance of Microsphere Resonators, *Sensors*, 2018, **18**, 2515.
- 96 M. Romanello, A. McGushin, C. Di Napoli, P. Drummond, N. Hughes, L. Jamart, H. Kennard, P. Lampard, B. S. Rodriguez, N. Arnell, S. Ayeb-Karlsson, K. Belesova, W. J. Cai, D. Campbell-Lendrum, S. Capstick, J. Chambers, L. Z. Chu, L. Ciampi, C. Dalin, N. Dasandi, S. Dasgupta, M. Davies, P. Dominguez-Salas, R. Dubrow, K. L. Ebi, M. Eckelman, P. Ekins, L. E. Escobar, L. Georgeson, D. Grace, H. Graham, S. H. Gunther, S. Hartinger, K. H. He, C. Heaviside, J. Hess, S. C. Hsu, S. Jankin, M. P. Jimenez, I. Kelman, G. Kiesewetter, P. L. Kinney, T. Kjellstrom, D. Kniveton, J. K. W. Lee, B. Lemke, Y. Liu, Z. Liu, M. Lott, R. Lowe, J. Martinez-

- Urtaza, M. Maslin, L. McAllister, C. McMichael, Z. F. Mi, J. Milner, K. Minor, N. Mohajeri, M. Moradi-Lakeh, K. Morrissey, S. Munzert, K. A. Murray, T. Neville, M. Nilsson, N. Obradovich, M. O. Sewe, T. Oreszczyń, M. Otto, F. Owfi, O. Pearman, D. Pencheon, M. Rabbaniha, E. Robinson, J. Rocklov, R. N. Salas, J. C. Semenza, J. Sherman, L. H. Shi, M. Springmann, M. Tabatabaei, J. Taylor, J. Trinanes, J. Shumake-Guillemot, B. Vu, F. Wagner, P. Wilkinson, M. Winning, M. Yglesias, S. H. Zhang, P. Gong, H. Montgomery, A. Costello and I. Hamilton, The 2021 report of the Lancet Countdown on health and climate change: code red for a healthy future, *Lancet*, 2021, **398**, 1619–1662.
- 97 H. Y. Li, H. J. Qi, J. F. Chang, P. P. Gai and F. Li, Recent progress in homogeneous electrochemical sensors and their designs and applications, *Trends Anal. Chem.*, 2022, **156**, 116712.
- 98 H. O. Kaya, A. E. Cetin, M. Azimzadeh and S. N. Topkaya, Pathogen detection with electrochemical biosensors: Advantages, challenges and future perspectives, *J. Electroanal. Chem.*, 2021, **882**, 114989.
- 99 H. Karimi-Maleh, H. Beitollahi, P. S. Kumar, S. Tajik, P. M. Jahani, F. Karimi, C. Karaman, Y. Vasseghian, M. Baghayeri, J. Rouhi, P. L. Show, S. Rajendran, L. Fu and N. Zare, Recent advances in carbon nanomaterials-based electrochemical sensors for food azo dyes detection, *Food Chem. Toxicol.*, 2022, **164**, 112961.
- 100 J. Sun, S. Abednatanzi, P. Van Der Voort, Y. Y. Liu and K. Leus, POM@MOF Hybrids: Synthesis and Applications, *Catalysts*, 2020, **10**, 578.
- 101 V. K. Abdelkader-Fernández, D. M. Fernandes, S. S. Balula, L. Cunha-Silva and C. Freire, Oxygen Evolution Reaction Electrocatalytic Improvement in POM@ZIF Nanocomposites: A Bidirectional Synergistic Effect, *ACS Appl. Energy Mater.*, 2020, **3**, 2925–2934.
- 102 C. Y. Zhao, H. Y. Ma, H. J. Pang, S. B. Li, Z. F. Zhang and Y. Yu, A new POMOF consisting of [VW12]<sub>4</sub> clusters and metal-organic nanotubes: Synthesis, structure, electrocatalytic and luminescent properties, *Inorg. Chem. Commun.*, 2016, **69**, 57–61.
- 103 S. Zhang, F. Ou, S. Ning and P. Cheng, Polyoxometalate-based metal-organic frameworks for heterogeneous catalysis, *Inorg. Chem. Front.*, 2021, **8**, 1865–1899.
- 104 X. M. Li, Y. M. Wang, Y. B. Mu, J. Liu, L. Zeng and Y. Q. Lan, Superprotonic Conductivity of a Functionalized Metal-Organic Framework at Ambient Conditions, *ACS Appl. Mater. Interfaces*, 2022, **14**, 9264–9271.
- 105 S. S. Li, L. Shang, B. L. Xu, S. H. Wang, K. Gu, Q. Y. Wu, Y. Sun, Q. H. Zhang, H. L. Yang, F. R. Zhang, L. Gu, T. R. Zhang and H. Y. Liu, A Nanozyme with Photo-Enhanced Dual Enzyme-Like Activities for Deep Pancreatic Cancer Therapy, *Angew. Chem., Int. Ed.*, 2019, **58**, 12754–12761.
- 106 B. Nasser, E. Alizadeh, F. Bani, S. Davaran, A. Akbarzadeh, N. Rabiee, A. Bahadori, M. Ziaei, M. Bagherzadeh, M. R. Saeb, M. Mozafari and M. R. Hamblin, Nanomaterials for photothermal and photodynamic cancer therapy, *Appl. Phys. Rev.*, 2022, **9**, 011317.
- 107 W. S. Yun, J. H. Park, D. K. Lim, C. H. Ahn, I. C. Sun and K. Kim, How Did Conventional Nanoparticle-Mediated Photothermal Therapy Become “Hot” in Combination with Cancer Immunotherapy?, *Cancers*, 2022, **14**, 2044.
- 108 C. Y. Cao, X. R. Wang, N. Yang, X. J. Song and X. C. Dong, Recent advances of cancer chemodynamic therapy based on Fenton/Fenton-like chemistry, *Chem. Sci.*, 2022, **13**, 863–889.
- 109 X. W. Wang, X. Y. Zhong, Z. Liu and L. Cheng, Recent progress of chemodynamic therapy-induced combination cancer therapy, *Nano Today*, 2020, **35**, 100946.
- 110 L. Ju, T. T. Mao, J. Malpica and T. Altan, Evaluation of Lubricants for Stamping of Al 5182-O Aluminum Sheet Using Cup Drawing Test, *J. Eng. Ind.*, 2015, **137**, 051010.
- 111 E. L. Zhang, X. T. Zhao, J. L. Hu, R. X. Wang, S. Fu and G. W. Qin, Antibacterial metals and alloys for potential biomedical implants, *Bioact. Mater.*, 2021, **6**, 2569–2612.
- 112 M. A. Kohanski, D. J. Dwyer and J. J. Collins, How antibiotics kill bacteria: from targets to networks, *Nat. Rev. Microbiol.*, 2010, **8**, 423–435.
- 113 M. Vecchiola, Antibiotic-resistant bugs in the 21st Century-A clinical super-challenge, *Rev. Chil. Infectol.*, 2009, **26**, 439–443.
- 114 W. Shin, H. S. Han, N. T. K. Le, K. Kang and H. Jang, Antibacterial nanoparticles: enhanced antibacterial efficiency of coral-like crystalline rhodium nanoplates, *RSC Adv.*, 2019, **9**, 6241–6244.
- 115 X. Chen, W. N. Shi, P. Liu, D. M. Xu and S. J. Sun, Development of molecular assays in the diagnosis of *Candida albicans* infections, *Ann. Microbiol.*, 2011, **61**, 403–409.
- 116 M. L. Tondo, R. Hurtado-Guerrero, E. A. Ceccarelli, M. Medina, E. G. Orellano and M. Martinez-Julvez, Crystal structure of the FAD-containing ferredoxin-NADP<sup>+</sup> reductase from the plant pathogen *Xanthomonas axonopodis* pv. *citri*, *BioMed Res. Int.*, 2013, 906572.
- 117 Y. Z. Xu, S. Y. Liu, L. L. Zeng, H. S. Ma, Y. F. Zhang, H. H. Yang, Y. C. Liu, S. Fang, J. Zhao, Y. S. Xu, C. R. Ashby, Y. L. He, Z. Dai and Y. H. Pan, An Enzyme-Engineered Nonporous Copper(I) Coordination Polymer Nanoplatfor for Cuproptosis-Based Synergistic Cancer Therapy, *Adv. Mater.*, 2022, **34**, 2204733.
- 118 M. Yari, M. B. Ghoshoon, B. Vakili and Y. Ghasemi, Therapeutic Enzymes: Applications and Approaches to Pharmacological Improvement, *Curr. Pharm. Biotechnol.*, 2017, **18**, 531–540.
- 119 G. Xu and H. L. McLeod, Strategies for enzyme/prodrug cancer therapy, *Clin. Cancer Res.*, 2001, **7**, 3314–3324.
- 120 L. S. Deng, Z. J. Jian, T. Xu, F. Q. Li, H. D. Deng, Y. C. Zhou, S. Y. Lai, Z. W. Xu and L. Zhu, Macrophage Polarization: An Important Candidate Regulator for Lung Diseases, *Molecules*, 2023, **28**, 2379.

- 121 Y. Q. Xia, L. Rao, H. M. Yao, Z. L. Wang, P. B. Ning and X. Y. Chen, Engineering Macrophages for Cancer Immunotherapy and Drug Delivery, *Adv. Mater.*, 2020, **32**, 2002054.
- 122 B. J. Langford, M. So, S. Raybardhan, V. Leung, J. P. R. Soucy, D. Westwood, N. Daneman and D. R. MacFadden, Antibiotic prescribing in patients with COVID-19: rapid review and meta-analysis, *Clin. Microbiol. Infect.*, 2021, **27**, 520–531.
- 123 C. Y. Du, Z. Zhang, G. L. Yu, H. P. Wu, H. Chen, L. Zhou, Y. Zhang, Y. H. Su, S. Y. Tan, L. Yang, J. H. Song and S. T. Wang, A review of metal organic framework (MOFs)-based materials for antibiotics removal via adsorption and photocatalysis, *Chemosphere*, 2021, **272**, 129501.
- 124 L. Fiorucci, F. Erba, R. Santucci and F. Sinibaldi, Cytochrome c Interaction with Cardiolipin Plays a Key Role in Cell Apoptosis: Implications for Human Diseases, *Symmetry*, 2022, **14**, 767.
- 125 W. J. Li, X. J. Luan, X. X. Zhu, J. Sun and L. L. Fan, Polyoxometalate embedded in metal-organic framework surface building strong polysulfides barrier for high-performance Li-S batteries, *J. Mater. Sci.*, 2022, **57**, 19946–19956.
- 126 S. Ul Hassan, S. Shafique, B. A. Palvasha, M. H. Saeed, S. A. R. Naqvi, S. Nadeem, S. Irfan, T. Akhter, A. L. Khan, M. S. Nazir, M. Hussain and Y. K. Park, Photocatalytic degradation of industrial dye using hybrid filler impregnated poly-sulfone membrane and optimizing the catalytic performance using Box-Behnken design, *Chemosphere*, 2023, **313**, 137418.
- 127 Y. Y. Dong, J. Zhang, Y. L. Yang, J. Q. Wang, B. Y. Hu, W. Wang, W. Cao, S. Gai, D. B. Xia, K. F. Lin and R. Q. Fan, Multifunctional nanostructured host-guest POM@MOF with lead sequestration capability induced stable and efficient perovskite solar cells, *Nano Energy*, 2022, **97**, 107184.
- 128 Z. W. Cui, J. F. Wu, Y. N. Xu, T. T. Wu, H. R. Li, J. Li, L. X. Kang, Y. H. Cai, J. Z. Li and D. Tian, In-situ growth of polyoxometalate-based metal-organic frameworks on wood as a promising dual-function filter for effective hazardous dye and iodine capture, *Chem. Eng. J.*, 2023, **451**, 138371.
- 129 F. Taghipour and M. Mirzaei, A survey of interactions in crystal structures of pyrazine-based compounds, *Acta Crystallogr., Sect. C: Struct. Chem.*, 2019, **75**, 231–247.
- 130 T. P. Vaid, S. P. Kelley and R. D. Rogers, Structure-directing effects of ionic liquids in the ionothermal synthesis of metal-organic frameworks, *IUCrJ*, 2017, **4**, 380–392.
- 131 M. Musa, D. M. Dawson, S. E. Ashbrook and R. E. Morris, Ionothermal synthesis and characterization of CoAPO-34 molecular sieve, *Microporous Mesoporous Mater.*, 2017, **239**, 336–341.
- 132 J. Y. Wang, W. Wu, H. Kondo, T. X. Fan and H. Zhou, Recent progress in microwave-assisted preparations of 2D materials and catalysis applications, *Nanotechnology*, 2022, **33**, 342002.
- 133 M. F. Elmahaishi, R. S. Azis, I. Ismail and F. D. Muhammad, A review on electromagnetic microwave absorption properties: their materials and performance, *J. Mater. Res. Technol.*, 2022, **20**, 2188–2220.
- 134 G. A. Tompsett, W. C. Conner and K. S. Yngvesson, Microwave synthesis of nanoporous materials, *ChemPhysChem*, 2006, **7**, 296–319.
- 135 D. Kumar, A. Joshi, G. Singh and R. K. Sharma, Polyoxometalate/ZIF-67 composite with exposed active sites as aqueous supercapacitor electrode, *Chem. Eng. J.*, 2022, **431**, 134085.
- 136 Y. W. Liu, B. X. Wang, Q. Fu, W. Liu, Y. Wang, L. Gu, D. S. Wang and Y. D. Li, Polyoxometalate-Based Metal-Organic Framework as Molecular Sieve for Highly Selective Semi-Hydrogenation of Acetylene on Isolated Single Pd Atom Sites, *Angew. Chem., Int. Ed.*, 2021, **60**, 22522–22528.
- 137 A. Blazevic and A. Rompel, The Anderson-Evans polyoxometalate: From inorganic building blocks via hybrid organic-inorganic structures to tomorrows “Bio-POM”, *Coord. Chem. Rev.*, 2016, **307**, 42–64.
- 138 D. Zang, Q. Li, G. Dai, M. Zeng, Y. Huang and Y. Wei, Interface engineering of Mo8/Cu heterostructures toward highly selective electrochemical reduction of carbon dioxide into acetate, *Appl. Catal., B*, 2021, **281**, 119426.
- 139 H. N. Miras, L. Vila-Nadal and L. Cronin, Polyoxometalate based open-frameworks (POM-OFs), *Chem. Soc. Rev.*, 2014, **43**, 5679–5699.
- 140 T. Wei, M. Zhang, P. Wu, Y. J. Tang, S. L. Li, F. C. Shen, X. L. Wang, X. P. Zhou and Y. Q. Lan, POM-based metal-organic framework/reduced graphene oxide nanocomposites with hybrid behavior of battery-supercapacitor for superior lithium storage, *Nano Energy*, 2017, **34**, 205–214.
- 141 T. G. Choleva, V. A. Gatselou, G. Z. Tsogas and D. L. Giokas, Intrinsic peroxidase-like activity of rhodium nanoparticles, and their application to the colorimetric determination of hydrogen peroxide and glucose, *Microchim. Acta*, 2018, **185**, 1–9.
- 142 Y. Li, M. W. Xie, X. P. Zhang, Q. Liu, D. M. Lin, C. G. Xu, F. Y. Xie and X. P. Sun, Co-MOF nanosheet array: A high-performance electrochemical sensor for non-enzymatic glucose detection, *Sens. Actuators, B*, 2019, **278**, 126–132.
- 143 Q. Q. Liu, Y. Zhong, H. Fu, R. Wang and L. H. Zhu, Synergy effect of highly dispersed palladium and Ni-SiW polyoxometalate-based metal-organic framework (POMOF) for highly efficient and selective nitroaromatics hydrogenation, *Appl. Catal., A*, 2023, **665**, 119373.
- 144 X. Q. Peng, S. S. Tang, D. T. Tang, D. W. Zhou, Y. Y. Li, Q. W. Chen, F. C. Wan, H. Lukas, H. Han, X. J. Zhang, W. Gao and S. Wu, Autonomous metal-organic framework nanorobots for active mitochondria-targeted cancer therapy, *Sci. Adv.*, 2023, **9**, eadh1736.



- 145 H. Yu, N. Ning, X. Meng, C. Chittasupho, L. L. Jiang and Y. Q. Zhao, Sequential Drug Delivery in Targeted Cancer Therapy, *Pharmaceutics*, 2022, **14**, 573.
- 146 S. F. Zhang, Y. H. Li, S. Sun, L. Liu, X. Y. Mu, S. H. Liu, M. L. Jiao, X. Z. Chen, K. Chen, H. Z. Ma, T. Li, X. Y. Liu, H. Wang, J. N. Zhang, J. Yang and X. D. Zhang, Single-atom nanozymes catalytically surpassing naturally occurring enzymes as sustained stitching for brain trauma, *Nat. Commun.*, 2022, **13**, 4744.
- 147 X. Y. Zhao, S. P. He, B. Li, B. Liu, Y. J. Shi, W. Cong, F. Gao, J. J. Li, F. Wang, K. Liu, C. Q. Sheng, J. J. Su and H. G. Hu, DUCNP@Mn-MOF/FOE as a Highly Selective and Bioavailable Drug Delivery System for Synergistic Combination Cancer Therapy, *Nano Lett.*, 2023, **23**, 863–871.
- 148 W. S. Ni, L. Zhang, H. R. Zhang, C. H. Zhang, K. Jiang and X. Y. Cao, Hierarchical MOF-on-MOF Architecture for pH/GSH-Controlled Drug Delivery and Fe-Based Chemodynamic Therapy, *Inorg. Chem.*, 2022, **61**, 3281–3287.
- 149 H. Y. Li, N. N. Lv, X. Li, B. T. Liu, J. Feng, X. H. Ren, T. Guo, D. W. Chen, J. F. Stoddart, R. Gref and J. W. Zhang, Composite CD-MOF nanocrystals-containing microspheres for sustained drug delivery, *Nanoscale*, 2017, **9**, 7454–7463.
- 150 I. A. Lazaro, C. J. R. Wells and R. S. Forgan, Multivariate Modulation of the Zr MOF UiO-66 for Defect-Controlled Combination Anticancer Drug Delivery, *Angew. Chem., Int. Ed.*, 2020, **59**, 5249–5255.
- 151 K. Suresh and A. J. Matzger, Enhanced Drug Delivery by Dissolution of Amorphous Drug Encapsulated in a Water Unstable Metal-Organic Framework (MOF), *Angew. Chem., Int. Ed.*, 2019, **58**, 16790–16794.
- 152 J. Yang, D. H. Dai, X. Zhang, L. S. Teng, L. J. Ma and Y. W. Yang, Multifunctional metal-organic framework (MOF)-based nanoplatfoms for cancer therapy: from single to combination therapy, *Theranostics*, 2023, **13**, 295.
- 153 X. L. Mu, Y. K. Zhong, T. Jiang and U. K. Cheang, Effect of solvation on the synthesis of MOF-based microrobots and their targeted-therapy applications, *Mater. Adv.*, 2021, **2**, 3871–3880.
- 154 B. Khezri and M. Pumera, Metal-Organic Frameworks Based Nano/Micro/Millimeter-Sized Self-Propelled Autonomous Machines, *Adv. Mater.*, 2019, **31**, 1806530.
- 155 P. Geng, N. Yu, D. K. Macharia, R. R. Meng, P. Qiu, C. Tao, M. Q. Li, H. J. Zhang, Z. G. Chen and W. S. Lian, MOF-derived CuS@Cu-MOF nanocomposites for synergistic photothermal-chemodynamic-chemo therapy, *Chem. Eng. J.*, 2022, **441**, 135964.